Chapter 7

Muon Detector

7.1 Introduction

The BTeV muon system has two primary functions:

- Muon identification: Many of the experiment's physics goals rely on efficient muon identification with excellent background rejection. Muon identification is important for rare decay searches, CP violation studies which require tagging, studies of beauty mixing, semileptonic decays, and searches for charm mixing.
- J/ψ and prompt muon trigger: Besides selecting interesting physics (including J/ψ final states of B decays, direct J/ψ production, and rare decays), this trigger performs an important service role by selecting a large enough sample of b events on which the more aggressive and technically challenging vertex trigger can be debugged and evaluated.

We have selected a toroidal magnet design combined with fine-grained tracking elements. This design permits a "stand-alone" trigger: *i.e.* a di-muon trigger based solely on information from the muon detector. In addition, improved background rejection is possible by comparing this measurement with momentum and tracking information from the rest of the spectrometer. The system design has been chosen to reduce and distribute occupancies and to minimize confusion in pattern recognition while allowing the muon trigger system to achieve a minimum bias rejection of about 500 with a di-muon efficiency of about 80%.

7.2 Muon System Overview

7.2.1 General design considerations

Given the objective of a stand-alone trigger and the size limitations set by the experimental hall, one can make fairly general calculations that place specific (and restrictive) constraints on the design of the system.

The fractional momentum resolution in a magnetic spectrometer can be parameterized as $\sigma_p/p = \sqrt{a^2 + (bp)^2}$ where the a term depends on the bending power and multiple scattering environment of the detectors and the b term depends on the bending power and the detector layout and spatial resolution. The detector layout is constrained by the size of the experimental hall. For a multiple scattering term of $a = 25\%$, a trigger with a minimum momentum requirement rejects low momentum muons at 4σ. The b term is important at high momentum, where it determines the fraction of high momentum tracks that fail a minimum momentum cut in a trigger. If b is less than 1%, the efficiency for high momentum tracks is very nearly one ($> 99\%$). Above 1%, the efficiency starts to fall off rapidly, approaching 70% for $b = 10\%$. Monte Carlo simulations of our design predict theoretical values for a and b of 19% and 0.6% respectively.

7.2.2 Baseline muon system

Two toroids, approximately 1 m long with 1.5 T fields, provide the bending power and filtering of non-muons. There will be three stations of detectors, one between the two toroids and two behind the toroids (farther from the interaction point in z), as shown in Fig. 7.1. The momentum of tracks can be measured using the two, well shielded, downstream stations and the nominal beam constraint. The station between the two toroids provides an important confirming hit for the rejection of fake tracks.

The basic building block in the construction of the a detector station is a "plank" of 3/8" diameter stainless steel proportional tubes. There are 32 tubes in each plank, arranged in two rows of 16 offset by half a tube diameter ("picket fence" style). (See Fig. 7.2.) These are held together with aluminum ribs and by the brass gas manifolds which are glued to the end of each plank. Each plank is a sturdy, self-supporting building block which acts as an excellent Faraday cage. We want to avoid ghost tracks in the system, so our minimum requirement is that all hits from one beam crossing be collected before the next beam crossing. A mixture of Ar-CO_2 meets this goal. The tubes will be strung with 30 μm diameter gold-plated tungsten wire, and the stainless steel tubes will have a wall thickness of 0.01". The 0.5 cm wire spacing of this design has no dead regions and has an effective spatial resolution of 1.4 mm.

To minimize occupancy at small radii, twelve planks of increasing length are arranged into pie shaped octants. To minimize pattern recognition confusion, three arrangement of planks (r, u, or v) are used. The r views are radial. The u and v views are rotated ± 22.5 degrees with respect to the radial views and measure the azimuthal angle, ϕ. A collection of 8 octants of like arrangement is called a view, and a collection of 4 views is called a station. In order to provide redundancy in the most important view in terms of pattern recognition for the trigger and momentum measurement, the r view is repeated in each station. The whole muon detector is three stations located at the end of the BTeV experiment, interspersed between and after magnetized iron toroids and shielding. A schematic of this arrangement is shown in Fig. 7.3.

The octants are the basic installation unit of the system. During the run, octants will

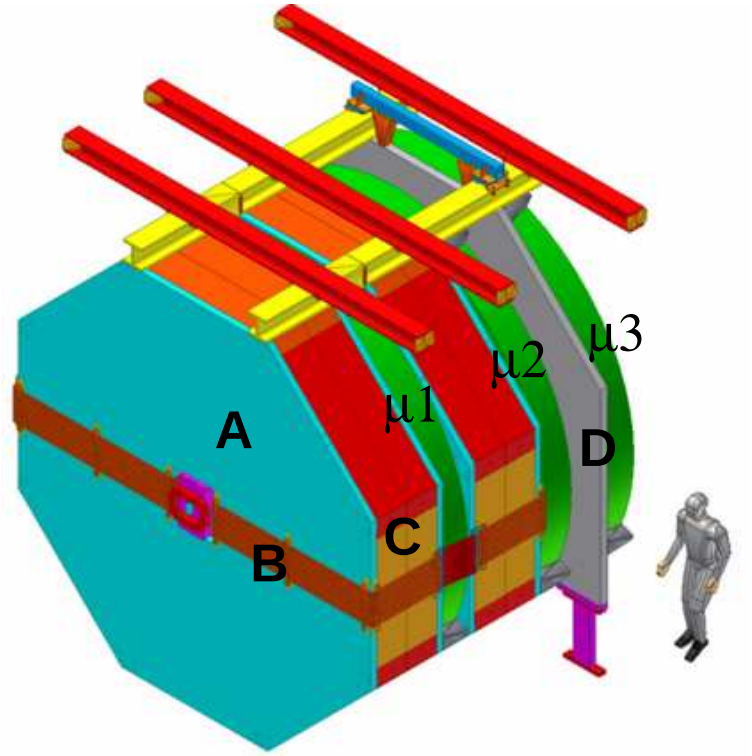

Figure 7.1: Perspective view of the Muon System of the BTeV spectrometer. From front to back, one can see: A, the smooth faceplate located on each side of each toroid, B, the coils which wrap around both toroids (the coils have a removable piece between the two toroids), C, the main steel for the first toroid, and D, the shielding wall located in front of the last muon station. The locations of the three muon detector stations are labeled "$\mu 1 - \mu 3$". Also shown is the compensating dipole in the center of the system.

be swapped in and out when the system requires maintenance. Bad planks in an octant will then be swapped out and fixed.

For a one-arm muon system, the 3 detector stations, with 4 views per station, 8 octants per view, and 12 planks per octant add up to a total of 1,152 planks or 36,864 tubes and electronics channels. (See Table 7.1.) The 8 octants in a view are mounted on two wheels, as described in Section 7.4.3. We will build one complete view (8 octants, 96 planks, 3,072 tubes) during the pre-production stage (which we will use to shake down and evaluate our production lines and methods). We will also make two additional views worth of planks to use as spares. These additional planks must be made at the same time to minimize the cost of the necessary parts and labor.

Figure 7.2: The basic building block of the muon system (plank). The inset shows an end view of the plank, and demonstrates the "picket fence" geometry of the proportional tubes. The gold colored pieces at each end of the plank are the brass gas manifolds. Visible at the end is the circuit board soldered around the edge to the brass piece.

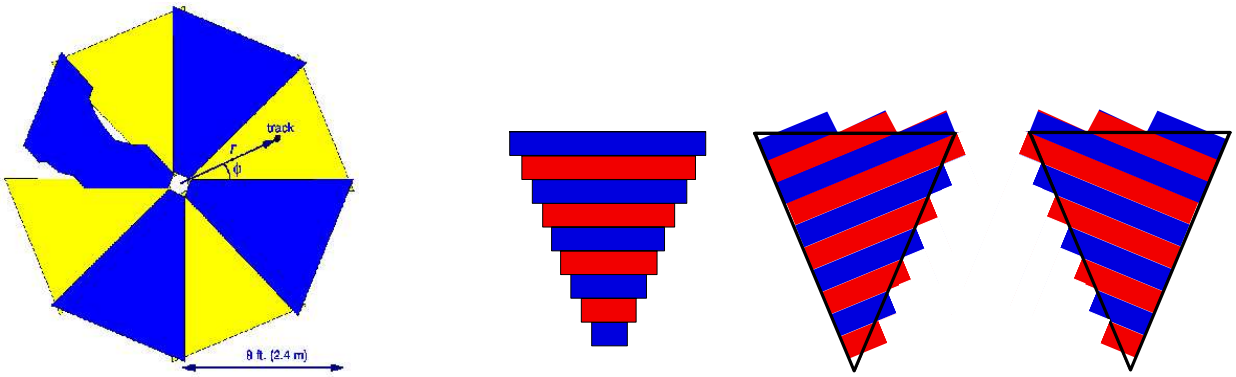

Figure 7.3: (left) Beams-eye view of one muon station (eight overlapping octants arranged in two layers). (right) Arrangement of planks to form each of the four views in an octant (r view is repeated). There will be 12 planks per octant (more than shown).

Item	**Number**
Stations	3
Views/station	4
Octants/view	8
Planks/octant (one view)	12
Tubes/plank	32
Total channels	36,864

Table 7.1: Channel and item counts for the BTeV muon system.

7.3 Requirements for the BTeV Muon System

The considerations that have gone into determining the requirements for the muon system include:

- The physics goals of the experiment
- The characteristics of both the events of interest and background events
- The physical size of the C0 hall and other detector components
- The robustness of the detector technologies
- Environmental, Safety, and Health (ES&H) issues

7.3.1 Physics requirements

These requirements are determined by the physics goals of BTeV.

1. **Luminosity:** The muon system must be able to operate at any bunch crossing time of 132 to 396 ns with a maximum luminosity of $4 \times 10^{32}(\mathrm{cm}^2\mathrm{s})^{-1}$.
2. **Lifetime:** The muon system must operate consistent with its design goals over the maximum lifetime of the experiment (10 years).
3. **Momentum resolution:** The "stand alone" momentum resolution of the muon system must be better than $\sigma_p/p = \sqrt{0.25^2 + (0.01p)^2}$.

7.3.2 Toroid requirements

1. **Bending power:** There should be two toroids in the (single) muon arm, each with a minimum field of 1.4 T and minimum thickness of 0.8 m.
2. **Magnetic field map:** The magnetic field must be known everywhere in the toroids to 1%.
3. **Magnetic field uniformity:** The magnetic field in each toroid must be uniform to 5%.

7.3.3 Proportional tube performance requirements

1. **Timing resolution:** The collection time for all proportional tube hits should be less than the beam crossing rate.
2. **Occupancy:** The maximum rate in any single proportional tube should be less than 200 kHz.

3. **Efficiency:** The typical efficiency of each proportional tube should be 98% or greater.

4. **Efficiency over lifetime:** The muon system efficiency over the lifetime of the experiment must be consistent with the BTeV physics goals. Currently it is thought that any aging effects will be negligible.

5. **Spatial resolution:** The position resolution of the proportional tube planks must be 2 mm or less.

7.3.4 Detector installation and support requirements

1. **Position reproducibility:** The position of the octants should be reproducible to 0.25 mm in x, y and z after they are moved (*e.g.* for maintenance).

2. **Removal/exchange:** The muon octant plates should be readily removable for maintenance. It must be possible to remove an octant during two 8 hour shifts, and replace an octant in two 8 hour shifts.

3. **Internal survey:** The coordinates of the individual muon proportional tubes within each octant needs to be known a priori to a level such that it does not contribute to the expected resolutions (2 mm) of the muon proportional tubes.

4. **External survey:** The coordinates of the station fiducials with respect to the BTeV absolute coordinate system needs be known a priori and maintained over the lifetime of the experiment. Final alignment transverse to the beamline and station position monitoring will be performed via software. The location of each station along the beamline (z) with respect to the experiment center must be determined within 2.3 mm over the face of the detector. The the station to station alignment, in terms of rotations about the beam axis, must be matched to within a milliradian (about a 2 mm shift around the rim of the detector). The station to station alignment, in terms of shifts transverse to the beam axis, must be matched within 2 mm.

5. **Flatness:** The center of a circular slice of a tube must not deviate by more than a perpendicular distance of 0.5 mm from the ideal long axis of symmetry. This is a requirement for wire stability at high voltage.

6. **Roundness:** The tube inner radius must not deviate by more than 0.5 mm towards the center of the tube from the ideal radius of the tube. This is a requirement for wire stability at high voltage.

7.3.5 Geometry requirements

These requirements are constrained by the size of the experimental hall.

1. **Station depth in z:** Each full detector station should not take more than 40.5 cm of space in z (the beam direction).

2. **Acceptance:** Each full detector station should cover radii between 38 cm and 240 cm.

7.3.6 Correction dipole requirements

1. **Installation interference:** The correction dipoles and their associated cabling should not restrict or interfere with the installation of the muon detector stations and their supporting infrastructure.

2. **Radial size:** The muon system needs to provide coverage down to 38 cm (Geometry requirement 2). The correction dipoles and their associated cabling should not restrict or interfere with this coverage.

7.3.7 Control and monitoring

1. **Environmental monitoring:** The muon system needs environmental monitoring (pressure and temperature). In order to be sensitive to 1/10th of the plateau region in the smallest plank (the best case), the monitoring must resolve a change equivalent to a change in HV of 10V or a change in gas gain of 1×10^4 (nominal gain is expected to be 1×10^5). This corresponds to 1/200th of an atmosphere and 1 degree C.

2. **Gas mixture monitoring:** We need to monitor the gas mixture for changes in mixture conditions equal to 0.1% (*e.g.* a change of a mixture of 85/15 Ar/CO_2 to 85.1/14.9).

3. **HV monitoring:** The muon system needs monitoring of the high voltage power supply voltage with a resolution of 2–3 V and current with a resolution of 0.1 μA.

4. **Gas gain monitoring:** The muon system requires monitoring of the gas gain and particularly needs to be alert to aging issues. The gas gain monitor must have a resolution equal to roughly 0.1% of the range of the plateau region, or, repeated samples of the gain over the course of a 24 hour period must produce a measurement of the derivative in the gas gain with a resolution of about 3×10^{-5}/(day), roughly 1×10^4/(life of the experiment).

5. **Gas contaminant monitoring:** The gas mixture must be monitored for contaminants with a gas mass spectrograph.

7.3.8 Software requirements

The software for the muon system refers to algorithms for track finding, monitoring systems, and diagnostic tools.

1. **Software standards:** Software development will conform to the *BTeV Software Standards*

2. **Muon Identification:** Muon identification software must be written which will perform track matching from the upstream spectrometer (a combination of pixel and straw tracks) to either hits or track segments in the muon system. The matching will be performed using the expected errors from the upstream spectrometer and the muon system and a confidence level will be assessed for the agreement. Where possible, an independent measurement of muon momentum will be calculated.

3. **Muon Calibration:** Software must be written to determine the geometry of the muon system and the efficiency of individual counters. These measurements will be estimated from data and included into the muon identification software at periodic intervals concurrent with significant changes in geometry or efficiency.

4. **Front End:** The programmable components in the front end electronics must have software capable of setting and verifying thresholds, pulsing sets of channels, sparsifying and gating the signals coming from the tubes, identifying the board electronically, and communicating with the slow control system. Additional functionality will be included to fully exploit the capabilities of the hardware (*e.g.* the ability to shut off a channel if we fully develop channel fusing).

5. **Monitoring:** Software must be developed to monitor changes in muon system performance using the data and to monitor changes in the physical environment of the detector (*e.g.* temperature, high voltage, current to the plank, pressure to an octant, gas flow to an octant, status of valves in the gas system, gas gain, gas impurities, gas mixing percentage, etc.). This software will have limits where operators will receive an alert if parameters exceed limits. Implicit in this requirement is an interface to BTeV DAQ for slow controls.

7.3.9 ES&H requirements

The muon system will have subsystems (electrical and gas handling), which could constitute safety hazards. The electrical will have sub-systems that have low voltage and high current, as well as high voltage and low current.

1. **Electrical safety:** All electrical aspects of the muon system will conform to the Fermilab ES&H manual on electrical safety.

2. **Gas handling safety:** All aspects of the gas handling system will conform to the Fermilab ES&H manual on gas systems.

7.3.10 Electrical requirements

1. **Compliance with BTeV Electronics Standards:** The muon system will comply with BTeV standards and the Fermilab ES&H manual on electrical safety.

7.3.11 Front-end electronics requirements

1. **Noise on FE:** The digital section of the front-end cards must not impact the performance of the analog portion, consistent with the physics goals of BTeV. The low and high voltage delivery must not impact the performance, consistent with the physics goals of BTeV.

2. **Thresholds:** Thresholds must extend from no higher than 0.1 fC to 16 fC with a resolution of 0.03 fC.

3. **Channel granularity:** The maximum number of channels to be controlled by a single threshold is 8.

4. **Channel control:** A common high voltage is to be sent to each plank.

5. **Fusing:** Fusing of low voltage will be done with fuses that self-recover.

7.3.12 Internal Interlocks

1. **HV over-current:** Individual high voltage channels must have a programmable over-current trip.

2. **HV interlock:** The high voltage system must have an interlock that prevents delivery of high voltage in the event of a need to shut off the system quickly.

3. **Gas interlock:** The gas system must have an interlock that prevents delivery of gas, or shunts the main delivery to either a known pure gas source or nitrogen, in the event of a need to shut off the main gas system quickly.

4. **LV interlock:** The low voltage system must have an interlock that prevents delivery of low voltage voltage in the event of a need to shut off the system quickly.

7.4 Technical Description

As shown in Fig. 7.1, two toroids, 1 m long with 1.5 T fields, provide the bending power. These toroids are described in detail in Section **??**. Additional information can also be found in Chapter **??**. The muon detectors will be set up in three stations, one between the toroids and two behind the toroids. The momentum can be measured using the two, well shielded, downstream stations and the nominal beam constraint. The station between the

two toroids ($\mu 1$) provides a powerful confirming hit to eliminate fake tracks. The geometry was chosen after careful consideration of many factors. Magnetizing both of the 1 m iron shields significantly improves momentum resolution which helps reduce background. The amount of iron shielding is selected to be the maximum allowed while still maintaining good angular coverage and fitting inside the C0 detector hall. Extra shielding was added near the third station after early GEANT simulations found high occupancies in that station. This extra shielding consists of 10 cm of iron shielding on either side of the third station plus a 5 cm thick collar around the beam pipe centered on the third station at a radius of 30–35 cm (just inside the muon detector).

The angular acceptance of the muon detector should ideally correspond to the acceptance of the spectrometer, which is 300 mr. However, the physical constraints of the experimental hall do not permit this. The detector radius is chosen to be as large as possible, 240 cm (nearly touching the floor of the enclosure), which corresponds to a polar angle acceptance at the last muon detector station of 200 mr. Fortunately, wider angle muons, which are outside of the acceptance of the muon detector, tend also to have lower energy and can be identified by the Ring Imaging Cherenkov detector (see Section **??**).

There are additional constraints on the inner radius of the detector. The BTeV analysis magnet is part of the Tevatron lattice and deflects the circulating beams. This deflection is compensated by dipole magnets at each end of the C0 enclosure. Moreover, the quadrupoles that focus the beam at the IR must be as close to the IR as possible. To achieve this, it has become necessary to save longitudinal space by inserting the compensating dipoles in the muon toroid as shown in Fig. 7.1. This defines the inner radius of the muon detector to be 38 cm, or about 40 mr. The presence of the magnet coils also creates potential for particle leakage which must be carefully shielded.

7.4.1 Muon detectors

The basic building block in the construction of a detector station is a **plank** of thin walled (0.01") 3/8" diameter stainless steel proportional tubes as shown in Fig. 7.2. Stainless steel was chosen because of its sturdy mechanical properties, its immunity to magnetic fields, and the fact that the oxide layer on stainless steel is conductive, which significantly reduces Malter effect.

Thirty-two tubes, arranged in a double layer with an offset of half a tube are glued (with a combination of conductive and structural epoxy in a two step process) at each end to a brass gas manifold and supported in the middle by brass rib pieces. A brass sheet is glued (with conductive epoxy) or spot welded to the brass manifold to maintain electrical continuity. This sheet is soldered to the circuit boards at each end of a plank. This design provides a sturdy, self-supporting building block which also acts as a Faraday cage to reduce external RF noise. Proportional tubes were selected because they are robust and have the necessary rate capability.

The 5.3 mm effective wire spacing of this design has an effective spatial resolution of

Radial coverage	38–240 cm
Full (3-station) polar angular coverage	40–200 mrad
Partial ($\geq$1-station) polar angular coverage	30–260 mrad
Toroid Z-locations (center)	870, 1010 cm
Station Z-locations (center)	942, 1082, 1197 cm
Total Length	4 m (includes toroids)
Toroid Length (each)	1 m
Toroidal Fields	1.5 T
Tube cell inner diameter	9.0 mm
Effective pitch:	5.3 mm
Spatial resolution	1.5 mm
Total channels	36,864
Momentum resolution	$\sigma_p/p = 19\% \oplus 0.6\% \times p$

Table 7.2: Parameters of the BTeV muon system.

5.3 mm/$\sqrt{12}$ = 1.5 mm with no dead regions between tubes. This meets our requirements for momentum resolution, drift time, and occupancy.

To minimize occupancy at small radii and improve pattern recognition, each detector station consists of eight overlapping pie shaped "octants," shown in Fig. 7.3. There are four views (r, u, v, and r) in each octant as shown in Fig. 7.3. The r (radial) view is repeated primarily to provide redundancy for the most important view in terms of momentum measurement and pattern recognition in the trigger (we require hits in 3 of 4 views to define a good muon in the trigger). It is possible though, to use the redundant r view as an aid for reconstructing track segments within a station. This allows us to make a more robust muon identification for two reasons: 1) very wide angle (characteristic of hadronic punch through) tracks which cause hits over several tubes in a plank can be mitigated with an additional view, and 2), the identification of wider angle, lower momentum, muons which fail to penetrate the entire system, can be performed with less misidentification. The u and v views are rotated $\pm 22.5^{\mathrm{O}}$ to measure ϕ and resolve hit ambiguities, reducing the misidentification rate. The basic installation unit of the system is an **octant** mounted on an octant plate. The octant is made of 12 planks and covers 1/8 of the azimuthal angle. Octants are mounted on octant plates which cover 1/4 of the azimuthal angle; thus two adjacent layers of octant plates (arranged in a wheel) provide full coverage for a single view.

A summary of the baseline BTeV muon system is given in Table 7.2. The total channel count comes from 3 stations $\times$ 4 views/station $\times$ 8 octants/view $\times$ 12 planks/octants $\times$ 32 tubes/plank = 36,864 channels.

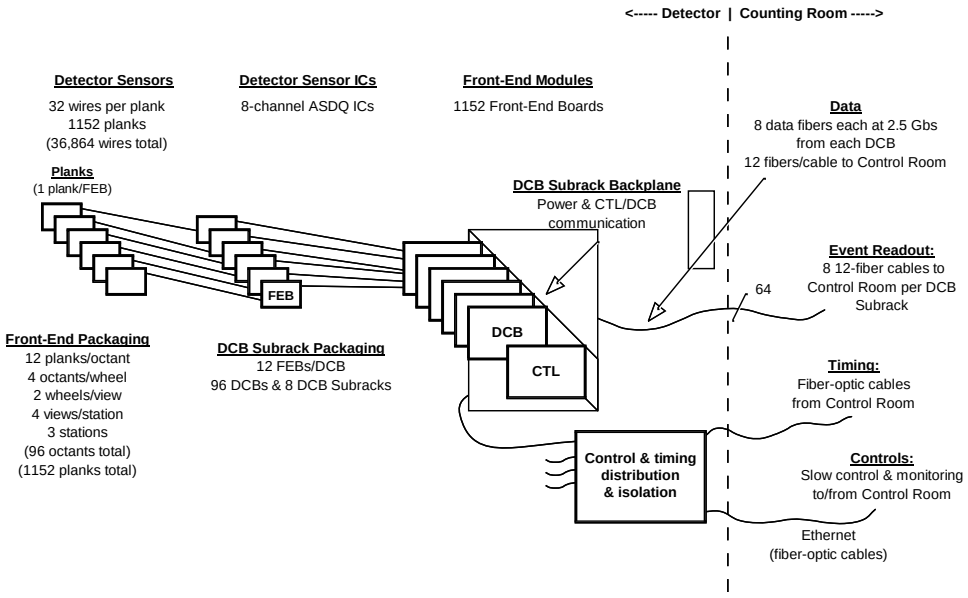

Figure 7.4: Block diagram of BTeV Muon Detector front-end electronics.

7.4.2 Front-end electronics

The front-end electronics will be similar to those used for the CDF central outer tracker (COT); circuit boards to deliver high voltage and a circuit board with electronics to amplify and digitize the tube signal. Both boards will be located at the end of each 32-channel plank.

We plan to use the ASDQ integrated circuit developed at the University of Pennsylvania to amplify and digitize the signals coming from the proportional tubes. This chip is used in the Run-II CDF COT for a similar purpose. The ASDQ, amplifies the first 8–10 ns of the the signal and outputs an LVDS signal. This chip, when mounted on a circuit board, has a low effective threshold of about $\sim$2 fC (confirmed by tests at Vanderbilt). The chip also features a double pulse resolution of $\sim$20 ns. The ASDQ digital signals will be sparsified, serialized, and read out on-board using the standard BTeV readout protocol. A fast copper link will transfer the data from the front-ends to a data control board (DCB). There will also be a serial link for slow control signals and a beam crossing clock sharing the same RJ-45 cable with the fast copper data link. A schematic diagram of the system is shown in Fig. 7.4

The design of the electronics emphasizes reduced noise. Less noise allows us to operate the tubes at a lower gain and gives us more headroom to increase gain if needed later. Lower gain means the tubes age more slowly. Having a broader gain control gives us more flexibility if we need to raise voltages. Since the ASDQ has a threshold control for 8 channels, we also have some flexibility within a plank for setting different gains and thresholds. This is especially true if our gas choice offers a wide plateau region for operating the plank at high efficiency (see Section 7.6.3).

Since the ASDQ chip will be common to both the muon and the straw systems, this production will be done in parallel with the straw detector. In the event that the process currently used to fabricated the ASDQ disappears, the design will be migrated to a new process. Funds for the migration, if needed, are included in the straw detector budget.

7.4.3 Mounting, support, and infrastructure

7.4.3.1 Mounting and support

The muon detector planks will be assembled octant modules prior to installation in the collision hall. Each module will be consist of planks sandwiched between two 1/8" aluminum plates, forming a "sealed" unit which contains cabling, etc. Four octant plates will be joined to form a "wheel" as they are installed about the correction dipole. Fig. 7.5 shows a stage in the installation process where the first plate is joined to a second plate. The resultant sections will then rotate on wheels placed around the circumference to make room for a third plate.

Fig. 7.6 shows some of the construction details for the radial octant plate, while Fig. 7.7 illustrates the method for attaching two plates during installation. As shown in Fig. 7.6, in order to leave room for electronics, cabling and gas piping, each wheel will include half of a given view. Hence each 4 view muon detector station will consist of 8 mounting wheels.

7.4.3.2 Gas system

We plan to use an Argon–CO_2 mixture, probably in the ratio 85:15. Gas studies at Vanderbilt have determined that this mixture provides a wide plateau region which makes it forgiving of variations in pressure, temperature, etc. This gas is also fast enough to ensure that ionization from adjacent beam crossings (a minimum 132 ns apart) will not be picked up with high efficiency. Finally, Ar–CO_2 is inorganic and does not suffer from hydrocarbon build up which is seen in high rate detectors which use organic gases, e.g. Argon–Ethane. Evidence for wire chamber aging in high-rate environments even with Ar–CO_2 has been found which is postulated to come from contaminants. We plan to minimize the contaminant problem in several ways. First, the entire gas system will be made of metal (copper, brass, and/or stainless steel) which is much more inert than plastic products. Second, we plan to test the delivered Argon and CO_2 gas. Third, we will monitor the gas gain continuously using a gas gain monitor with an Fe-55 source as shown in Fig. 7.8. Finally, we will use a gas mass spectrograph to check the mixing and to check for impurities in the gas.

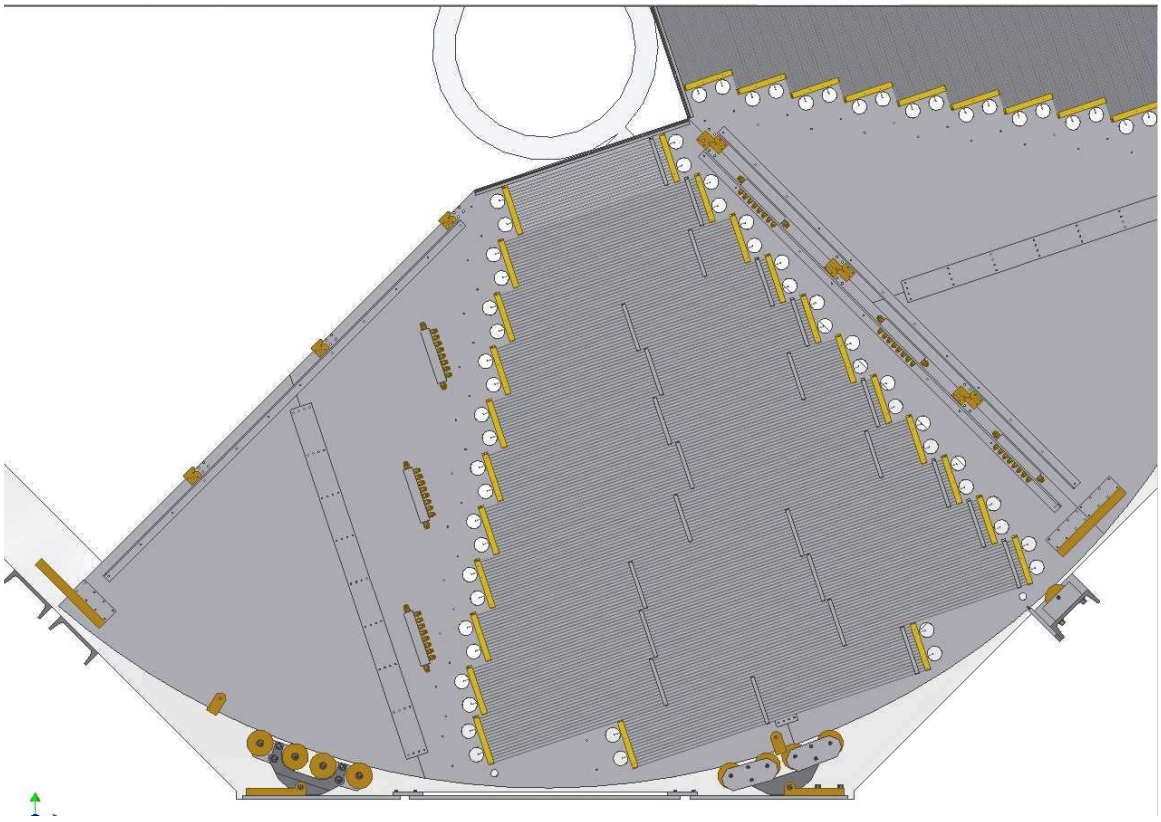

Figure 7.5: Two octant modules are in position to be joined together. The lower two wheels system are arranged to form a locomotive "bogie" and bear all of the weight during the installation process. The system rotates on a set of wheels placed at the circumference. After the first two modules are joined, the two-module system is rolled into a position to allow for the installation of the third module.

The gas system starts with pure Argon and CO_2 which are mixed in a mixing system. The gas flow is split several times in several different manifolds until reaching the planks. Gas flow will be completely parallel, that is, no gas will go through more than one plank. The gas system will be designed to allow up to 5 gas volume exchanges per day in the plank closest to the beam (about 3.5 liters/min). We show the design for the gas mixing system in Fig. 7.9 and the design for the overall gas system in Fig. 7.10.

We will also utilize gas gain monitors to monitor the gas gain over time. These will be placed at the input and output ends of the gas system and will be composed of single tubes and an Fe-55 source.

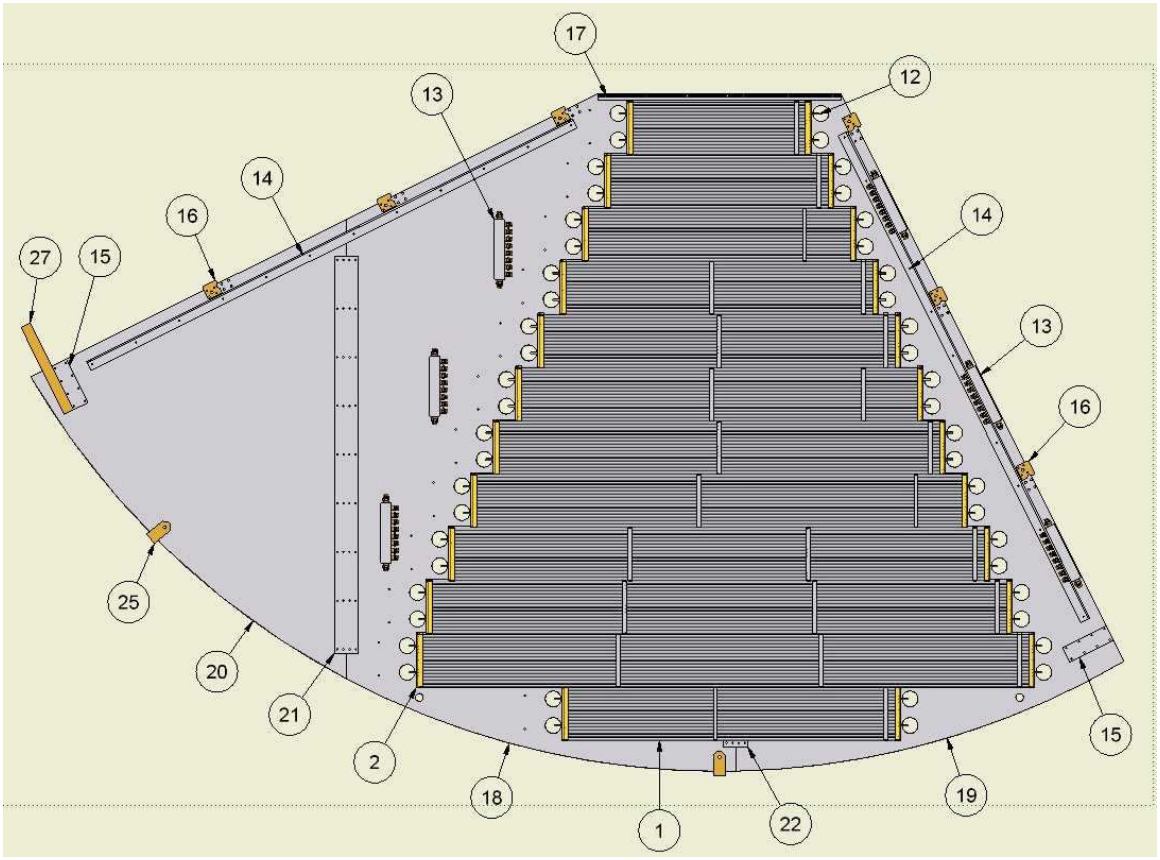

Figure 7.6: Assembly details of a radial octant plate. Each 1/4" thick radial plate is constructed out of three sections that are joined together using joint-bars (part 21 and 22). The blank area to the left of the tubes will be used for gas and electronics access. Gas will be distributed from three manifold assemblies (part 13). Stiffening-angles (part 14) are included to inhibit the bending of the octant plate during installation. The radial edges of this plate and adjacent plate are connected by knitting- brackets (part 15) and tie-bars (part 27).

7.4.3.3 High and low voltage

A controllable high voltage will be delivered to each plank, and the current will be monitored on all 1,152 channels. The high voltage system will be capable of delivering sufficient current so that the highest rate tubes near the beam will not lose performance. We are currently looking at a high voltage system from CAEN which is a candidate for use by several detectors. We expect to have a maximum voltage need of 1750 V and a maximum current needed of 2 μA. The front-end boards need power for both the ASDQ's and the FPGA/digital portion of the front end board. We have measured the the amount of power required when the combined analog and digital board was being driven at its maximum expected signal rate. Since the amount of power each plank uses, 2.5 W, is fairly small, our design uses linear

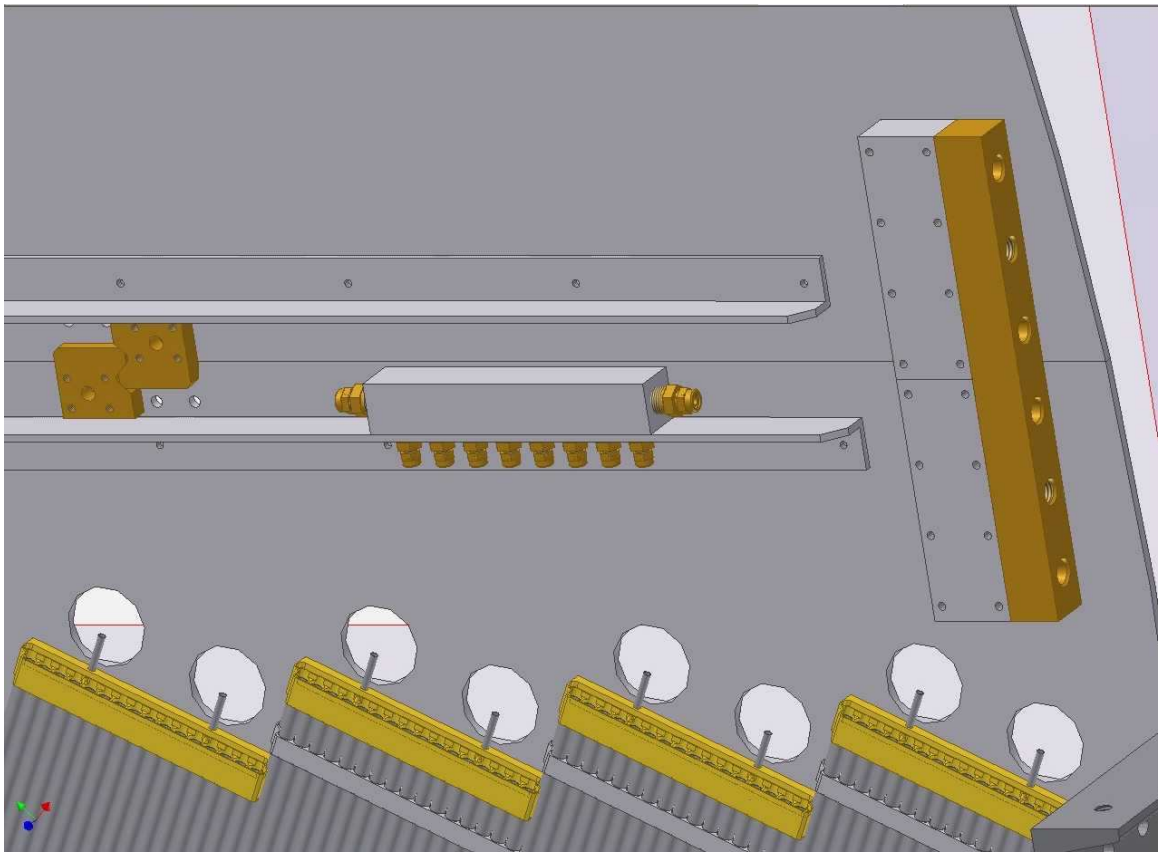

Figure 7.7: We show details of how the plates are joined together as the mounting wheel is constructed. The "knitting-brackets" impede relative radial motion between the two plates and are overlapped to impede motion transverse to the plate plane. The tie-bar prevents one plate from folding about two radial edges that join. We also show more details of the manifold assembly and stiffening-angles. The tie-bar consists of 1.25" by 1.25" square brass bar. The radial stiffening-angle also extends 1.25" from the surface of the plate. Once a wheel is assembled, it will be supported from the lift blocks (part 25) as illustrated by Fig. 7.24. We have holes in the plate near each gas connection to the plank manifold to allow us to accommodate the width of the gas fitting.

power supplies and a straightforward distribution network to deliver the low voltage to each plank. Although the present low voltage design is fairly complete for the muon system, the collaboration is exploring common solutions for all the detectors requiring low voltage.

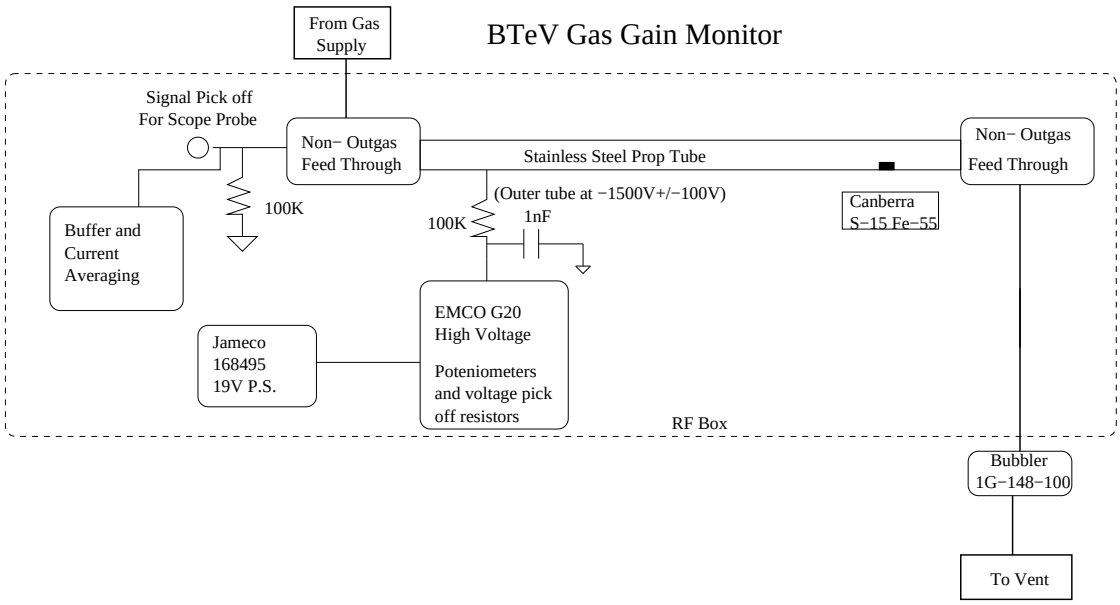

Figure 7.8: Design of gas gain monitor for the muon detector in the BTeV experiment.

7.5 Design trade-offs

7.5.1 Magnetized vs. non-magnetized toroids

The BTeV muon system has the two goals of providing clean off-line identification of muon tracks as well as providing an complementary trigger to the main BTeV detached vertex trigger. We believe that the only way to achieve adequate rejection for this complementary trigger is to select $J/\psi \rightarrow \mu^+\mu^-$ candidates by requiring two opposite sign, moderate momentum penetrating particles. We further believe that the ability to make a redundant momentum measurement of a muon candidate in the muon system will significantly reduce misidentification of hadrons due to their in-flight decay prior to entering the muon filter.

In the early phases of the muon system design, we investigated the possibility of exploiting the magnetic dispersion of the central dipole to make a momentum measurement by extrapolating the hits in the muon system to the nominal beam collision center. We were unable to achieve a fractional momentum resolution much better than a constant $\sigma_p/p = 200\%$ with any of the possible detector scenarios considered. About 1/3 of the momentum smearing came from the event-by-event variation of the interaction point, and 2/3 came from substantial multiple scattering in the electromagnetic calorimetry and the steel hadronic absorbers themselves. The fundamental problem was the effective dipole bend center was too far upstream of the multiple scattering sources to make a useful momentum measurement.

These considerations lead us to consider the momentum resolution achievable using a magnetized toroid. Again the momentum measurement would be derived by extrapolating the measured track trajectory in the muon system through the magnetic toroid and central

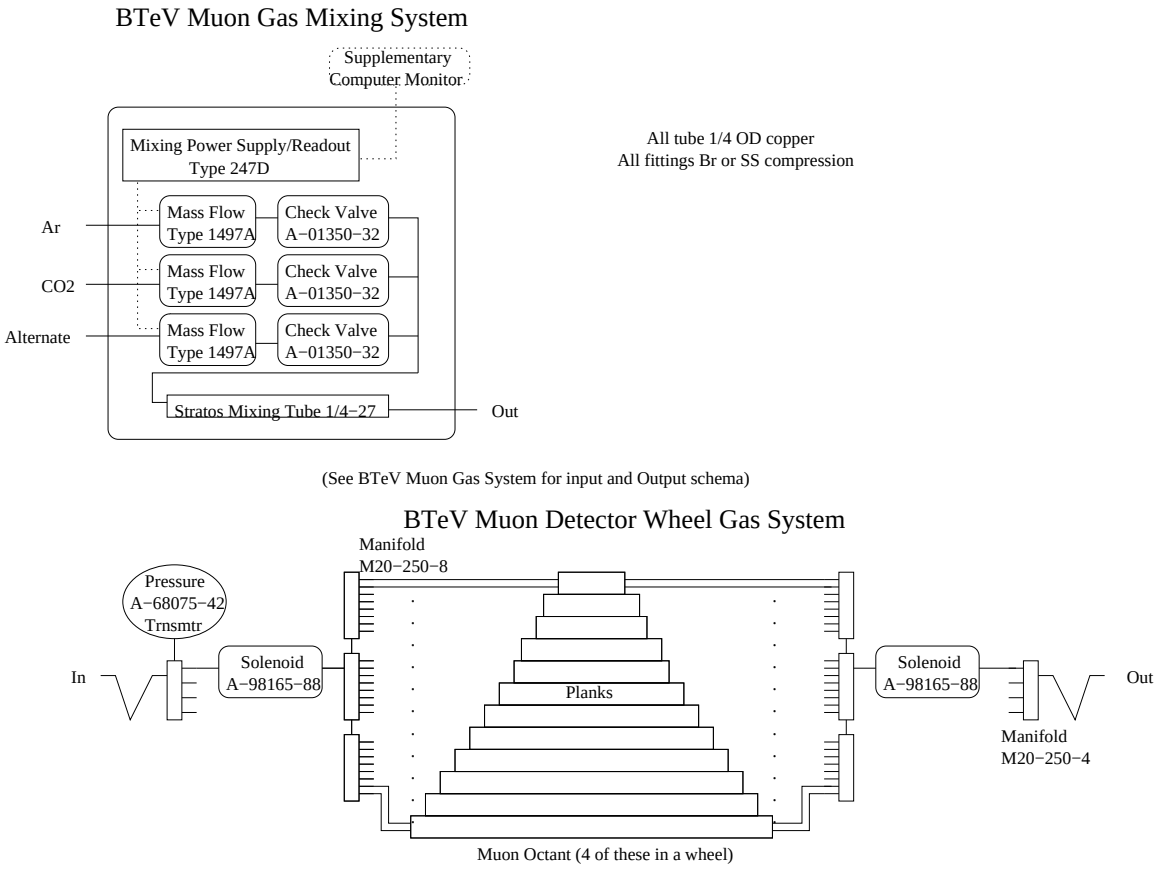

Figure 7.9: The design of the gas mixing system (left), and the delivery schema to the collection of detector planks on an octant.

dipole to a nominal beam center. We found a single 1 meter thick saturated toroid provided insufficient bending power to produce a suitable trigger. In particular, the fractional momentum resolution of such a single magnetized toroid system would vary from 25 to 40% depending on the azimuth of the muon track. Essentially, the bending power of the central dipole would "fight" the bending power of toroid because of their different field geometries. We finally settled on the present design that has two one meter thick magnetized toroids and three measurement stations. This layout produces a fairly uniform fractional momentum resolution of better than 20% over the full momentum range relevant to $J/\psi \rightarrow \mu^+\mu^-$ in BTeV given the intrinsic spacial resolution of our proportional tubes.

See BTeV-doc-970 [1] for an early, but more thorough, exploration of toroid and shielding possibilities.

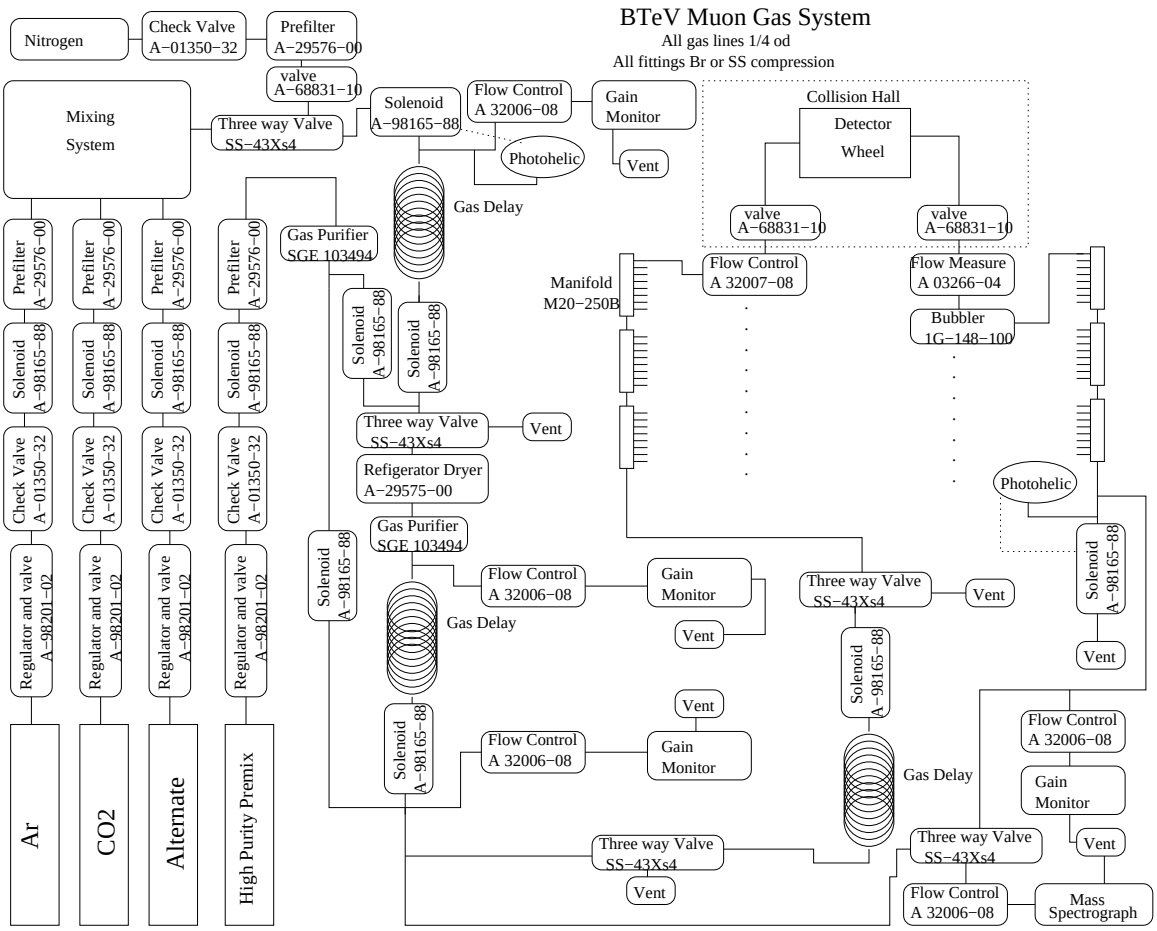

Figure 7.10: The overall design of the gas system. There are redundant layers of monitoring and delivery.

7.6 Past Research and Development Work

7.6.1 Summer 1999 beam test

In the spring of 1999, we constructed 10 planks of varying lengths (see below). These were transported to Fermilab in June for a test beam run. A stand on which the planks could be mounted was designed and built to allow the planks to be rotated and offset. The front-end electronics were sample ASD8B cards from the University of Pennsylvania which provided amplification, shaping, and discriminating of the signal from the proportional tubes. Testing these boards revealed a high susceptibility to ambient RF noise. To reduce this noise, boxes to enclose the electronics were constructed out of circuit board and wrapped in copper tape. Interface cards to provide high voltage to the tubes and low voltage to the electronics were designed and assembled. An interface card to convert the LVDS signal, output by the ASD8B

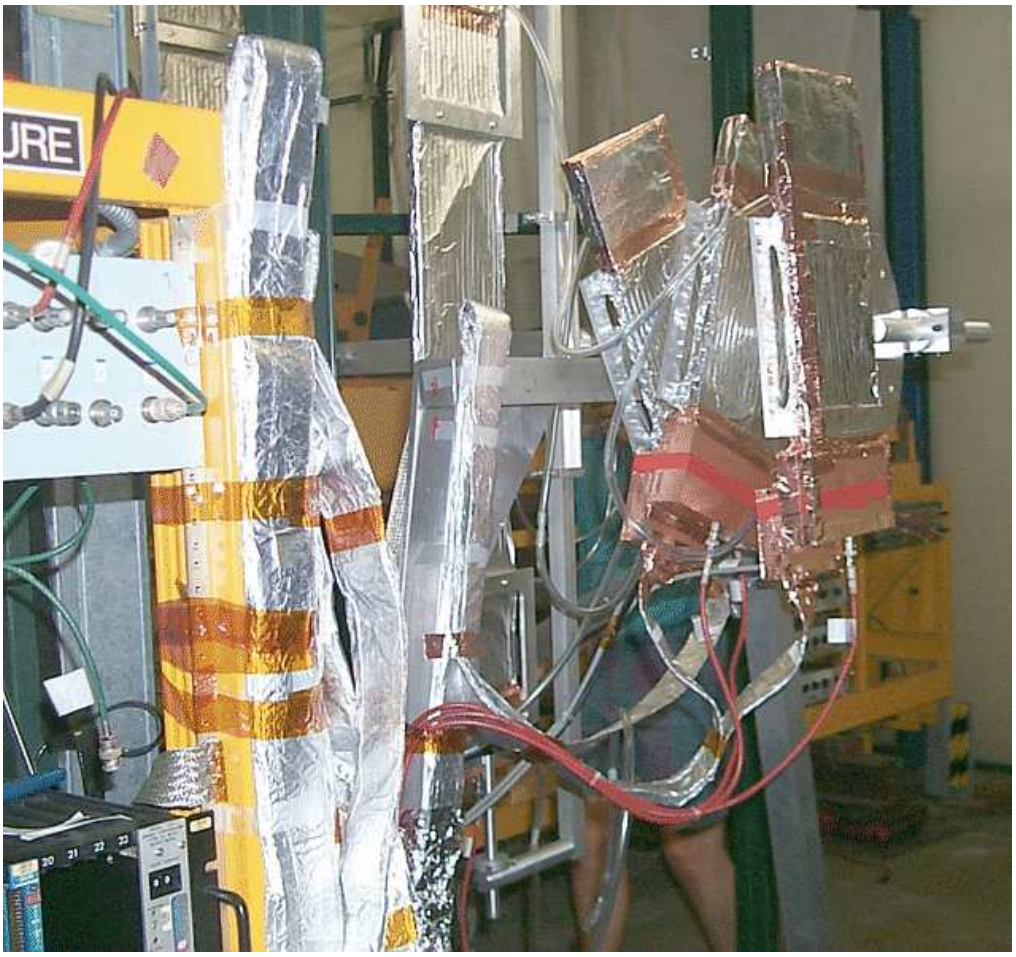

Figure 7.11: The BTeV muon system setup for the 1999 test beam run. Five planks are visible in this photograph. Noise problems required shielding with aluminum foil and copper tape.

card, to ECL was also designed and built. The muon data acquisition system was written using a CAMAC interface. The TDC data from the planks and the latches from the trigger scintillators were recorded. Reconstruction software and an online event display were written in order to interpret the data. The detector setup can be seen in Fig. 7.11. As a result of our experience in this test beam, several changes were made to the original plank mechanical and electrical design.

7.6.2 Plank design/construction

The first round of plank prototypes (10 planks of 32 tubes) were constructed in 1999. These planks were constructed (see BTeV-doc-991 [2]) in the following way:

1. Tubes were cut to length in the machine shop from purchased stock.

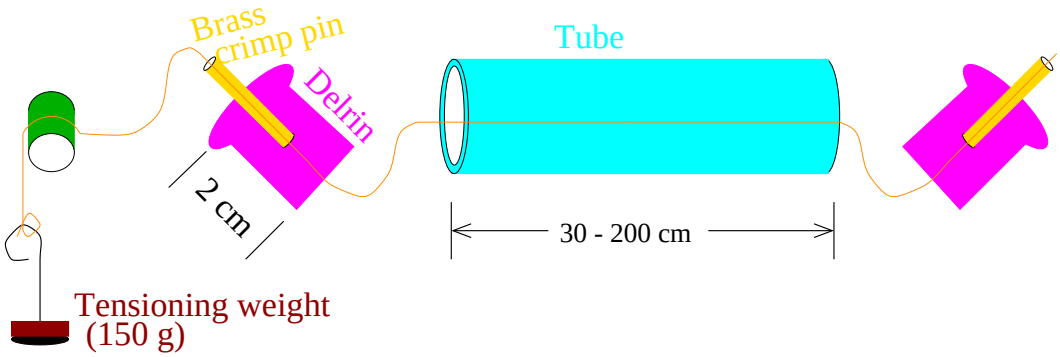

Figure 7.12: Diagram of the stringing process.

2. Each tube was cleaned in an Alconox solution, rinsed, and dried with compressed air.

3. As shown in Fig. 7.12, a gold-plated tungsten wire was strung through a Delrin insert on one end of the tube, through the tube, and through another Delrin insert. The Delrin insert consists of a tubular piece of Delrin with a lip at one end to hold it at the edge of a tube. A hole drilled through the center of the Delrin contains a small brass tube (crimp pin) extending out. The brass crimp pin for this prototype contained a double funnel inside to center the wire (a function now included in the Delrin insert which allows us to use a stock brass tube for a crimp pin). Each Delrin insert also had three small holes for gas flow.

4. After stringing, one end of the tube was crimped. The Delrin insert was inserted into the tube. Then a resistor lead was inserted in the brass crimp pin (along with the wire) and a commercial crimp tool was used to crimp everything together.

5. After crimping one end, the other end was attached to a calibrated weight to achieve the proper tension and the other end was crimped.

6. Continuity and high voltage tests on each tube ensured the crimp held and the wire did not break.

7. A plank was constructed from 32 strung tubes. The endcaps were machined from Noryl (plastic) and contained one hole for gas and 32 small holes for the end of the crimp pins (which connect to the electronics). The endcaps were glued to the end of planks.

The construction of 10 planks in the spring of 1999 provided us with valuable information. We found that 30 μm and 50 μm wire both work well while the 20 μm wire was harder to string and was not needed for the muon system. We found that one crimp often did not hold the wire in place while two crimps were almost always sufficient. The crimp was also not airtight requiring glue or solder on the end of the crimp pins to ensure a good seal.

In the summer 1999 beam test, plateau curves showed that the planks were >95% efficient at 1.8 kV for a 30 μm wire with Ar–CO_2 gas. This agreed with our expectations. However,

cross talk between channels was very high which resulted in many tubes in a plank firing with only one incident particle. This prevented us from measuring individual tube efficiency or position resolution.

The susceptibility to external noise and extensive cross talk led to several design changes. The ASDQ (one of the successors to the ASD8B chip used in the beam test) was selected for the real muon system. Tests have shown this chip to be more resistant to external RF noise. We also redesigned the high voltage distribution card to reduce crosstalk. Finally, the plank design was changed to use a brass manifold, instead of plastic, which was soldered to the stainless steel tubes to provide a Faraday cage. These modifications solved the cross talk and external noise problems. The changes to the design also required changes in plank construction. Since the Delrin insert might melt or slip during the soldering process, the tubes were strung after soldering the brass manifold. A new homemade crimp tool was created to work in the restricted space available. Another change was the creation of an aluminum box to contain the electronics. This box bolts to the brass manifold, providing the last part of the Faraday cage.

Prototypes of the new design were then fabricated, and problems were encountered with the stringing process: crimps with the new tool were not as reliable and the entire process took significantly more time. Therefore, we made a final change to the design. We went back to stringing the tubes individually, then gluing them into the gas manifolds instead of soldering. To provide electrical continuity, conductive epoxy is used between the tubes and the manifold. (Structural epoxy is used to provide the mechanical strength.) A brass sheet is then glued (with conductive epoxy) or spot welded to the gas manifold and soldered to the circuit boards at the end of a plank after the main assembly and gluing are completed.

7.6.3 Plank and gas tests

A prototype plank of the latest type has been made and tested. This plank as well as three of the previous iteration (brass manifold soldered to the tubes) are seen in a cosmic ray test stand in Fig. 7.13. The latest design incorporates the new plank construction, a CDF central outer tracker front-end card with ASDQ chips, and a redesigned high-voltage distribution card. Results from the cosmic ray test stand indicate a tube efficiency greater than 99%. The noise level is very near the theoretical minimum (the 2 fC of the ASDQ chip).

A variety of Argon–CO_2 gas mixtures were tested in the cosmic ray test setup. The gas gain results for several mixtures of Ar–CO_2 are plotted versus voltage in Fig. 7.14. These gains were obtained using an Fe-55 source. Also shown in Fig. 7.14 are plateau curves for an Ar–CO_2 mixture of 85:15; the current choice for the muon system. Fig. 7.15 shows the spread in first arrival times of hits in a plank with an Ar–CO_2 mixture of 85:15. The spread is found to be about 100 ns, fast enough to run with a minimum possible Tevatron bunch crossing time of 132 ns, and even better suited to a longer Tevatron clock due to the after pulsing effects (about 15% of tracks produce an extra pulse beyond 100 ns, 2% beyond 200 ns, etc.) present in Ar–CO_2.

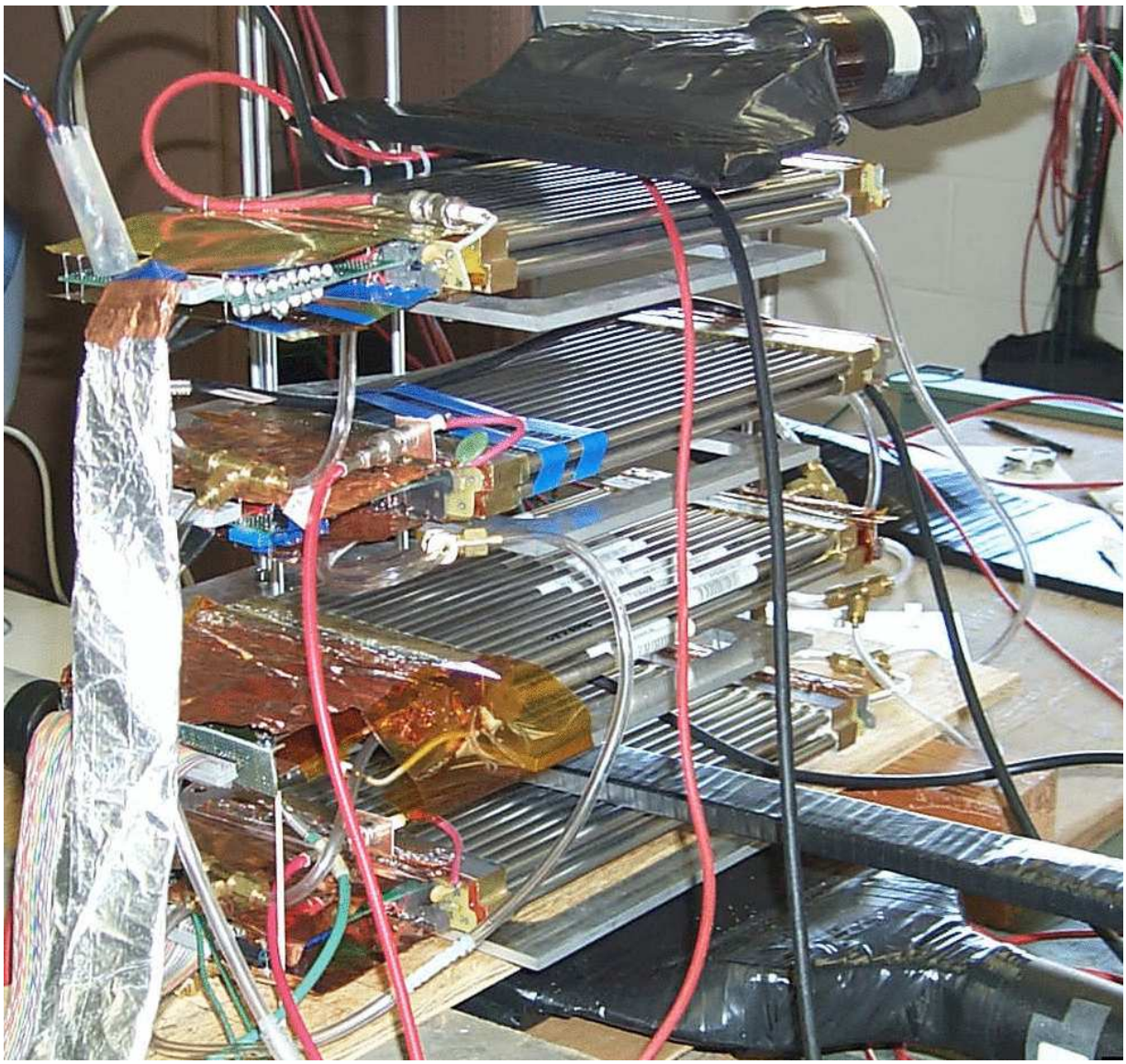

Figure 7.13: Photograph of the muon system cosmic ray test stand with four planks and several scintillators.

7.6.4 Construction database

We have developed a database system to collect and track information during detector construction and commissioning. As each detector element is constructed or tested, the relevant information will be entered into the database for later retrieval and correlation studies. A single database will be used by all institutions working on the BTeV muon system. Each proportional tube, electronics board, and larger items will have a bar code attached for easy tracking. Also, all raw materials used in the construction of the detector will be tracked from source to final location.

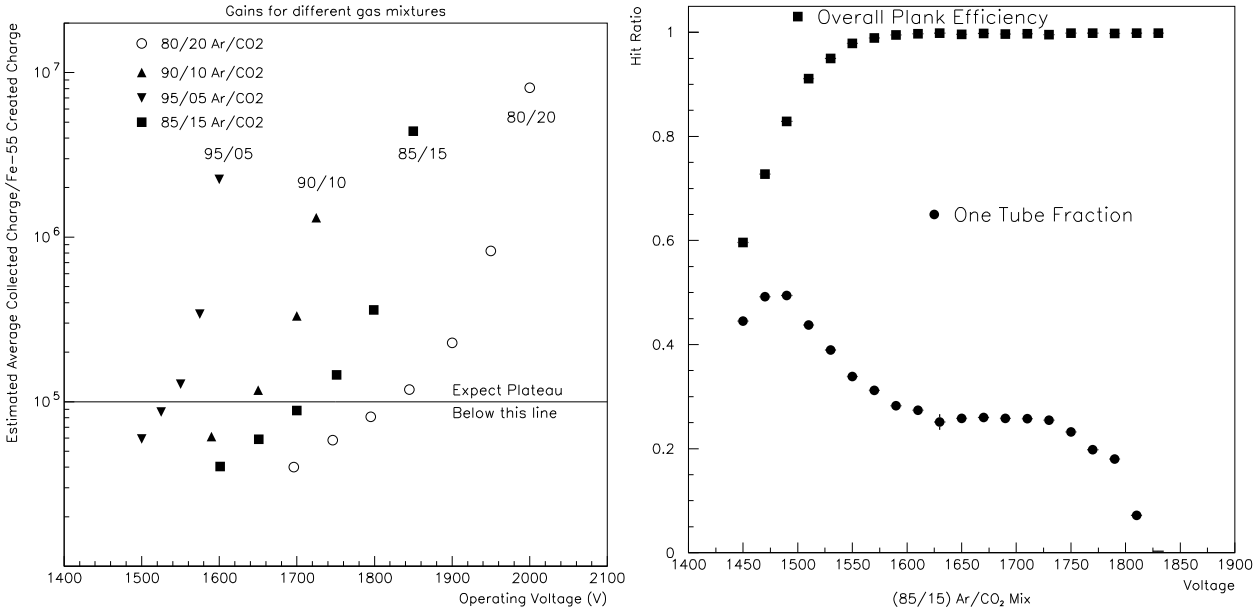

Figure 7.14: Left: measured gain of various mixtures of $\mathrm{Ar}\,\mathrm{CO}_2$ versus voltage. Right: plateau curves for 85:15 mixture of Ar–CO_2; the top curve shows plank efficiency versus voltage and the bottom curve shows the ratio of single hits to all hits. A broad plateau region is observed in the region of 1600 V to 1750 V.

7.6.5 Wire tension measurement

To ensure that each tube is strung with a wire of the correct tension, the tension of each wire is measured by placing the plank in a magnetic field, driving the wire with a sinusoidal current, and measuring the induced EMF to find the resonant frequency. From this value the tension is computed. We have developed a test stand which automatically measures the tensions in a plank full of tubes and stores the resulting information in the construction tracking database.

7.6.6 Detector construction and support

In the process of developing installation and support plans for the muon system we developed a 1/5 scale model of the muon system shown in Fig. 7.16. This model also includes the muon detector environment such as walls and toroids. In our initial plan, the muon planks would be mounted on quad plates which would then be hoisted into position using a series of overhead winch manipulations. Based on our experiences with this model, we concluded that installation as well as disassembly for repair would take a prohibitively long time since many separate hoisting manipulations were required. For this reason, we developed the new plan described in Section 7.4.3.

The octant mounting scheme has been redesigned to provide greater stability and ease of assembly. Two thinner sheets of aluminum are used rather than one sheet for mounting and

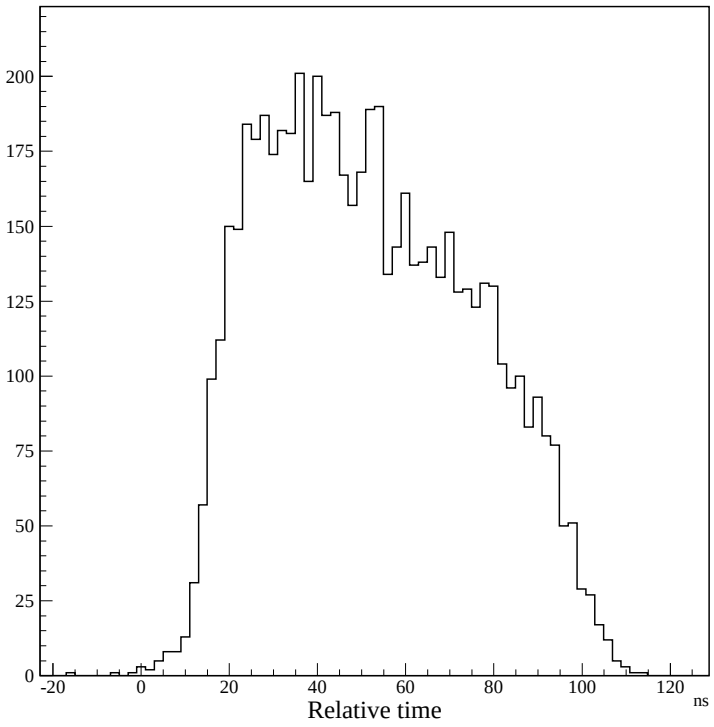

Figure 7.15: Arrival times of the *first* hits in a plank of proportional tubes (relative to an independent trigger) in a cosmic ray test stand. The spread is less than the anticipated 132 ns (fastest) bunch crossing time of the Tevatron, and robust for a gas with some after pulsing, like Ar–CO_2, for a longer Tevatron clock.

stiffening bars are included; both add strength and rigidity to the octant module. Further, the cable and gas connections have been simplified to allow fast connect/disconnect in the case of a dipole replacement. The new design allows us to construct just one "flavor" of electronics as well. This means the the orientation of readout and termination are constant with respect to a plank, and less circuit board types need to be produced. A view of the proposed new octant design is shown in Figure 7.17.

A full-sized mockup of a single wheel (there are eight wheels per station) has been created and assembled by University of Illinois personnel. The first installation test was done with a wheel where extra weight to simulate the planks was *not* present in the wheel. Assembling the entire wheel required less than four hours of labor. The completed structure is shown in Figure 7.18. This configuration weighs about 60% of the final (with planks) configuration, so the additional weight is not considered to be a problem. Another test with a fully weighted wheel will be performed soon.

A survey of the flatness of the wheel, as installed, was performed [3]. Improvements on the flatness are expected with improved stiffener bars and rigidity supplied by the installed planks.

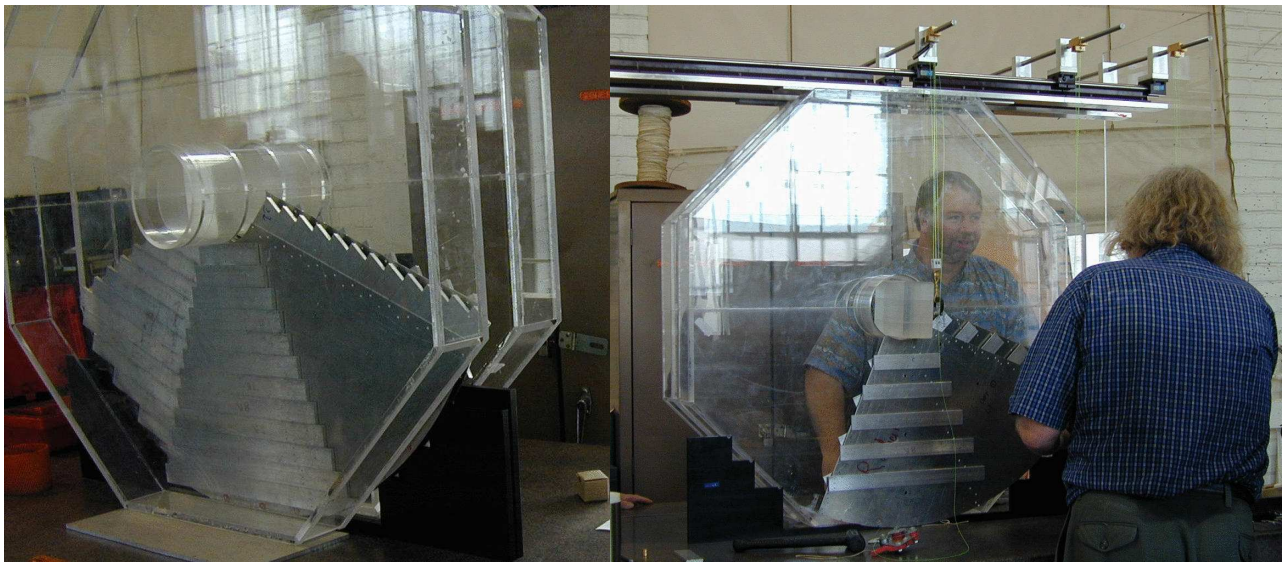

Figure 7.16: Photographs of the 1/5-scale model of the original mounting scheme. Left: two quads, back to back, between the Plexiglas toroids. Right: view showing the overhead support and installation system.

7.6.7 Front-end electronics

Since we are using the muon system in the trigger, and we want to separate beam crossings, we chose our electronics to react to the leading edge of the signal from the proportional tube. We have chosen to use the ASDQ chip to accomplish the fast analog to digital conversion of the proportional tube signal. This chip or its variants are a popular choice for tracking, and our group has a long experience with using this chip family successfully. The straw detector is using the chip as well and BTeV is committed to transferring the chip to a new process if needed, though at present (Spring 2004) Maxim does not plan to obsolete the process for the ASDQ in the foreseeable future. There has been a conversion of the process used for the ASDQ, Cpi, from 4 in. to 6 in. wafers, but Maxim has waived the expense for conversion of the ASDQ.

Each plank is a self contained data acquisition and control unit. This means that the front end board on the plank has extensive digital functionality. It also means that there is a potential to induce significant noise into the analog portion of the board. In our determination of the gas mixture to use, we used a board that was originally designed for the CDF Central Outer Tracker (COT). This board contained no digital functionality other than discriminator output of the ASDQ. We were able to operate the COT card with our prototype plank at an efficiency exceeding 99% with a signal threshold that was slightly better than the specification for the "average" ASDQ chip. These tests are detailed in the gas section. Melding the ASDQ COT card successfully with extensive digital circuitry at the location of the detector was our primary concern in our prototyping efforts.

In Fig. 7.20 we show the board diagram for the noise and functionality tests performed at

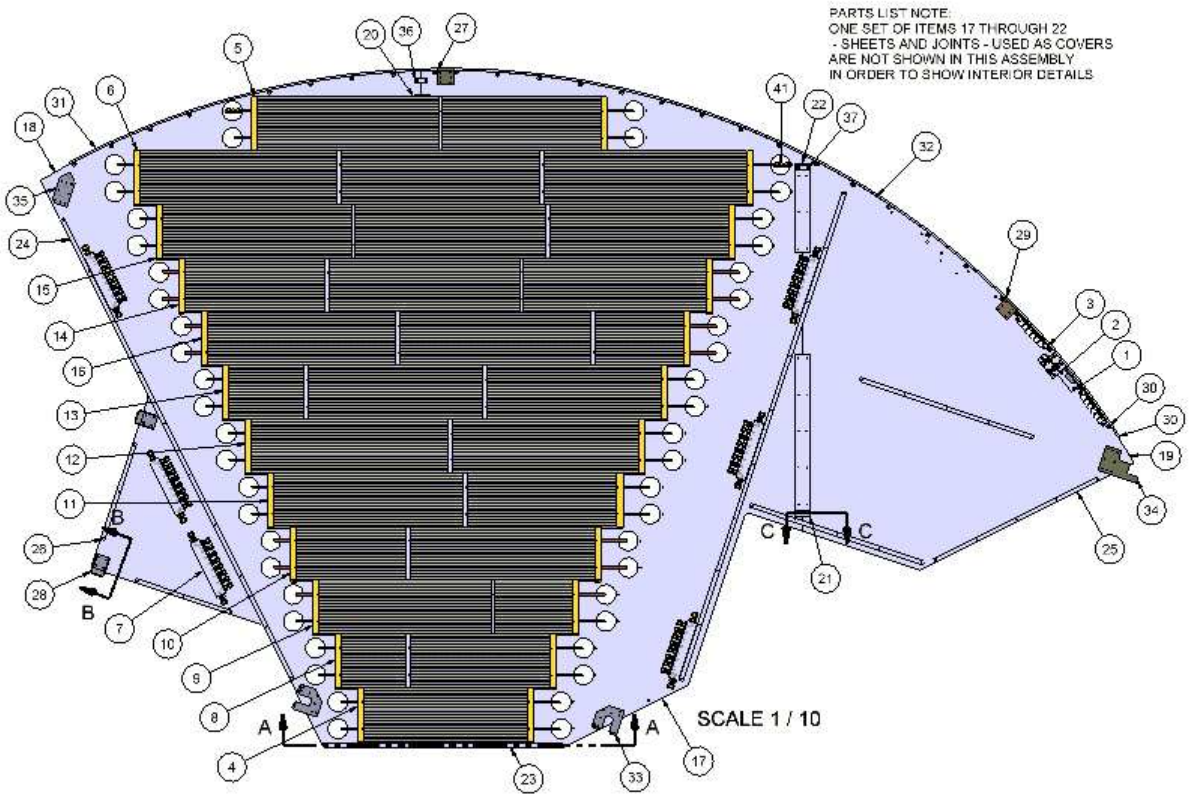

Figure 7.17: A cutaway view of the new octant design. Note the additional locking and guiding features located at 33, for instance, in the figure. Also note the clustering of services such as gas, HV, LV etc. at the upper right hand side.

Fermilab in the spring and summer of 2002. In the tests it was important to determine that the new card performed as well as the COT card while delivering on the promise of digital functionality. In tests without the muon detector attached, a threshold of 2 fC was attained with less than 1 Hz of noise. This is similar to the performance of our plank prototype with the COT card.

The tests performed were rather extreme. Digital traces were placed on the board and connected to unused I/O pins of the FPGA. These lines were exercised while we looked at the output of the ASDQ. When we attached a muon plank to the prototype front end board (see Fig. 7.21) we had to increase the threshold from 2 fC to 2.5 fC to maintain 1 Hz/channel noise at 100% (pulser) efficiency. Subsequently, we discovered that the threshold could be lowered by removing a kludge that was made to the threshold circuitry. We also connected a scintillation counter trigger in coincidence and demonstrated that the board could be triggered (see Fig. 7.22). A side benefit of this test was the determination that the leading edge of the signal coming from the ASDQ can be localized to within 5 ns of the trigger

Figure 7.18: A full sized mockup of a muon detector mounting wheel. Built and installed at the University of Illinois.

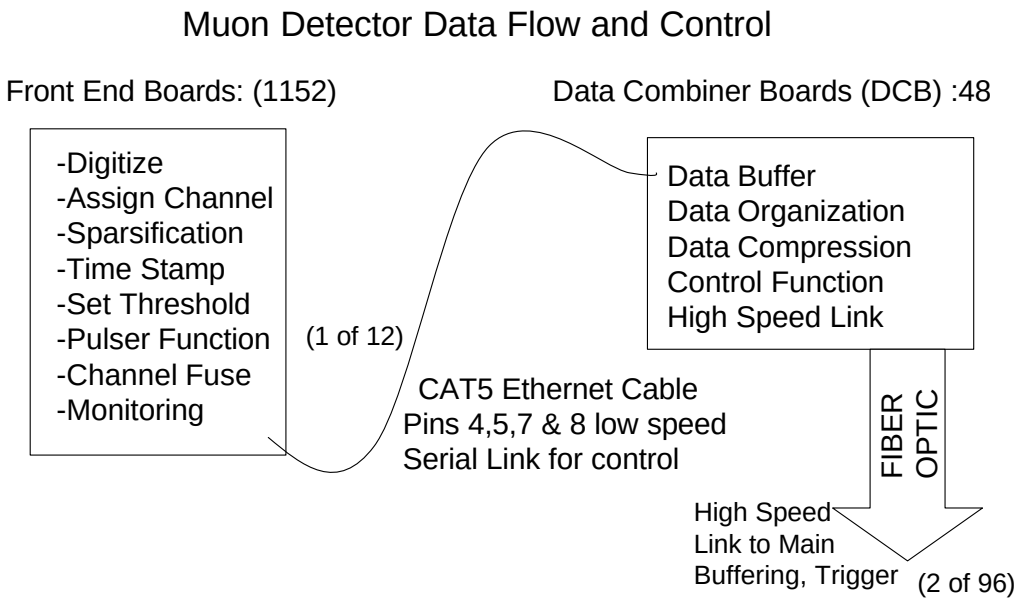

Figure 7.19: Diagram outlining the functions of the Front-End board and the data combiner board. The connection between the boards is done via commercially available CAT-5 cable. We intend to use the "dark wire" in this standard as a low speed serial link. Sparsified data with a time stamp will be sent via the high speed link, while control and monitoring functions will be done via the slow link.

signal. This makes it possible to add tube correlations in addition to selecting an acceptance window to the FPGA programming.

The conclusion from the testing of the prototype with digital readout is that this approach works well.

7.7 Planned Research and Development Work

We will continue gas gain and plank efficiency measurements in our cosmic ray test stand. Refinements of the plank construction will also be investigated in hopes of finding a method which reduces the construction time while maintaining the needed features.

7.7.1 MTEST beam test

We plan to construct 3–5 more planks to test during the beam test in the summer-winter of 2004. This test run will allow us to perform many of the studies which we were unable to make in 1999 due to noise problems. These studies include measuring speeds and responses of various gasses, measuring high rate effects, and measuring individual tube efficiency and

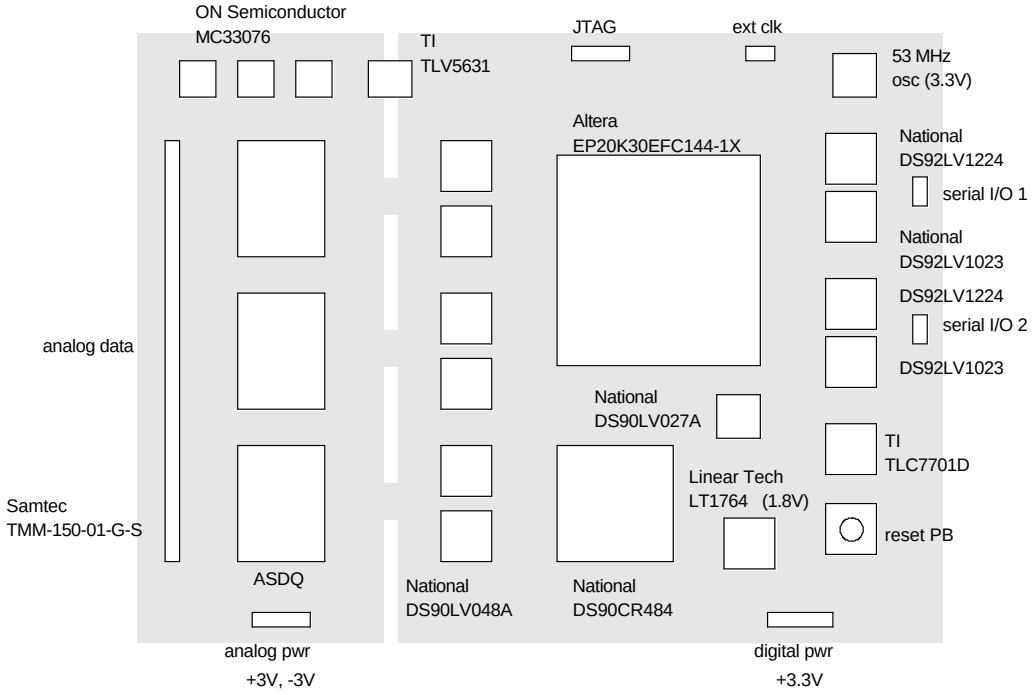

Figure 7.20: Circuit Board diagram for the prototype electronics of the muon detector. The board is actually overloaded to perform noise and transmitter studies. Notice that this board is designed to operate with LVTTL logic, while the actual production board will make extensive use of LVDS logic. LVDS is the natural output of the ASDQ chip and is an inherently low noise logic standard.

resolution. We expect the results of these tests to validate our design changes. We have already installed a high precision silicon tracker to help facilitate our (and other groups) beam tests.

7.7.2 High dose test

We plan to perform a high dose test of our detector to check for problems with the materials we are using in the construction of our detector. We need to perform this test as soon as possible, in case design changes are needed.

We would like to put a plank somewhere in the Tevatron or Booster where it will receive a high dose of particles from beam backgrounds. Many materials have problems with outgassing after such exposures, and the only way to be absolutely sure that our materials will not have problems is to check them. We would also run gas through the plank (with electronics) at a rate commensurate with our plans for actual running conditions, and mon-

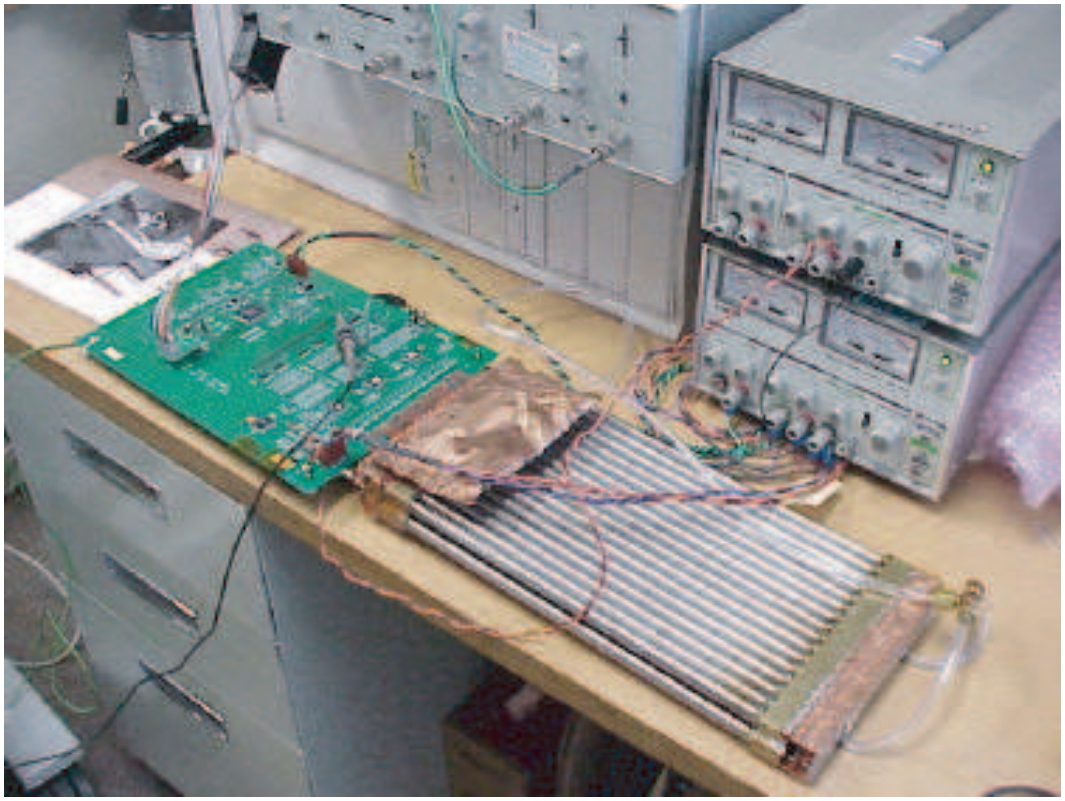

Figure 7.21: Front End prototype hooked up to a prototype plank. Notice especially the unsophisticated nature of the power delivery, the digital I/O, and the lack of an RF enclosure for the board. We find that the robust nature of the design is present in systems of several planks as well. We are hoping that this will offer us us some latitude in making final design choices that can both ease construction and lower cost without compromising performance.

itor the plank. We may also connect high voltage and if so we will need to monitor current draws, etc.

7.7.3 Prototype electronics and plank interface

Later in the design process, we will make a pre-production prototype containing the actual electronic components we will use in the production. We feel it is premature at this stage to finalize the design of the digital portion of the board. Commercial chips come and go with remarkable volatility, and we want to be able to take advantage of the best choices when we are prepared to build the production electronics.

We have been investigating different materials for the electrical connection between the tubes and the readout electronics. In preliminary studies, we have had a great success using conductive epoxy Tra Duct 2902 as a replacement for soldering the tubes to the gas

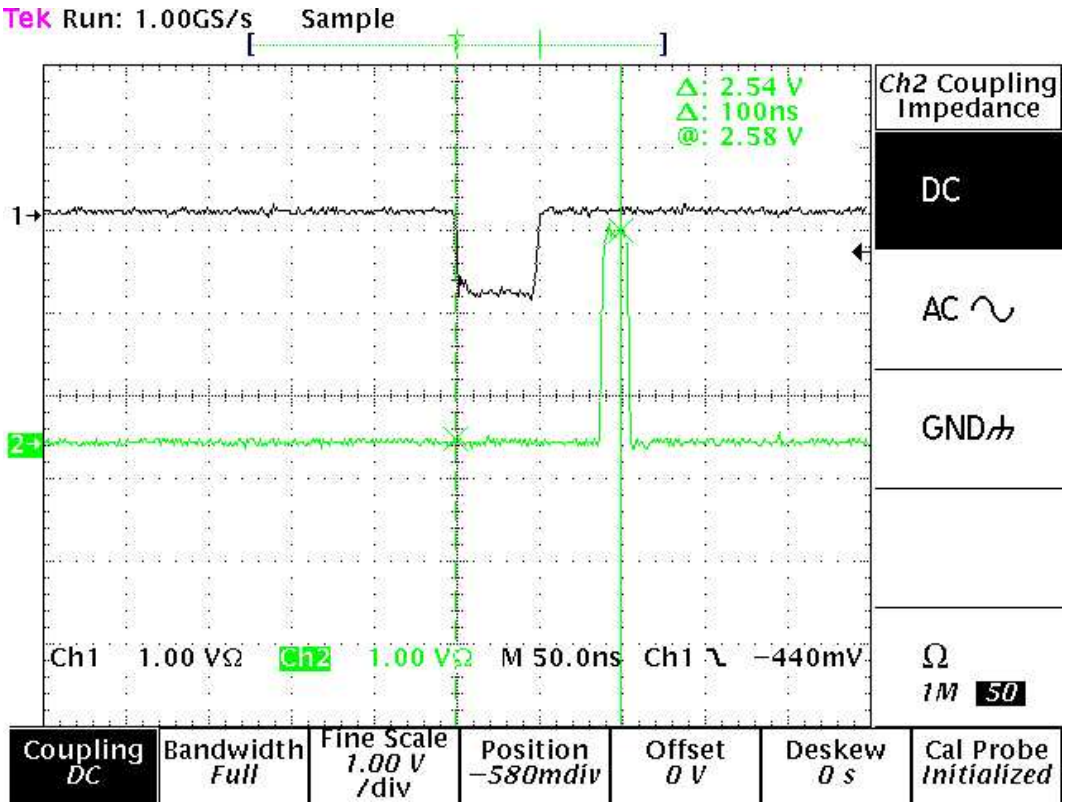

Figure 7.22: Output of the "or" of the connected plank channels (bottom trace 2) of the front end board prototype in response to a cosmic ray trigger(top trace 1).

manifolds. This epoxy is known to be chamber friendly and is being used by the straws and many LHC experiments. We are also trying to replace the conducting sheet that connects the gas manifold and the readout electronics with a conductive rubber gasket. This gasket material has been employed successfully in the CDF experiment for many years and would facilitate a very easy connection. This is important as it allows us some more flexibility in how we schedule the delivery of components. I.e. a completed plank need not be wedded to its final electronics until just prior to being installed in an octant.

7.7.4 Mechanical refinements and tests

We plan on testing several design changes which address difficulties in the current design. Illinois has redesigned the gas manifold to allow a plank to be restrung if needed. This will not be a simple procedure, but it will at least be possible. Also included in the redesign of the gas manifold are provisions for easier machining of the gas inlet, more brass for a connection to a conductive gasket, and extra brass to allow for epoxy potting and greater mechanical strength.

Figure 7.23: Test rig for looking at wire stability at high voltage for one of our long (6 ft.) planks.

The central rib design has been simplified and moved to aluminum.

We have tested the calculations related to wire stability with a test jig. We find our flatness requirement over the face of an octant to be adequate. Figure 7.23 is a picture of the setup used to measure wire stability.

7.7.5 Octant test stand

One important aspect of our quality and assurance plan is a test stand capable of fully testing all aspects of an octant. This includes checks of the gas, high voltage, and low voltage systems, as well as a check of the readout of all detector channels and their electronics. We want to design, build, test, and iterate a prototype test stand. Based on this experience we will finalize the design of the octant test stand.

We will purchase readout electronics, high voltage and low voltage supplies, and gas system components. For the readout, we will design and build a relatively simple board that consists of 8 fiber receivers and 8 data buffers. This card will be read out by a DSP card that plugs into the PCI bus on a PC. This card has been designed by colleagues at Vanderbilt who will build one for us and let us use their software.

We plan to assemble the prototype test stand prior to building the pre-production octants. We will test, debug and improve our design during the 4–5 month period in which these octants come together. Planks will be fabricated at each university site (Illinois, Puerto Rico–Mayaguez, and Vanderbilt), shipped to the pre-production assembly site at Illinois, and gradually assembled into the pre-production octants. Whether these octants will form mounting wheels (we will have enough for two) or a quadrant (1/4 of the azimuthal angle in each station with some redundancy) of the full detector for combined tracking tests or some combination of the two is still to be determined.

7.7.6 Plank construction jig

We will be designing an adjustable jig which will be used to maintain precise tube lengths and properly orient the gas manifolds with respect to the tubes and mounting plates during the assembly process. Such a jig is required to efficiently assemble the large number of tubes of many different lengths with adequate precision to allow us to mount the array in the confined space available.

7.7.7 Prototype gas system

During the running of BTeV, we plan to carefully monitor our gas mixture. Given our high rate environment, aging of our system is a significant concern. We need to monitor our gas supply carefully to verify that it does not contain dangerous levels of contaminants (hydrocarbons, water, etc.). We will therefore continually monitor the gas gain using a small test chamber and Fe-55 source, and will use a gas mass spectrograph to check the mixture ratio and to check for impurities. In order to gain experience with this hardware, and develop our methods and procedures, we plan to procure the necessary components and test them thoroughly.

7.7.8 C0 background studies

We would like to build a system of detectors to install in the C0 hall, and use them to measure background rates. While the beam conditions will not be identical to those during BTeV running, our measurements can be compared to calculations and used as a check of those calculations.

For these studies, we plan to reuse the muon scintillator counters from the fixed-target experiment FOCUS. These counters were built and operated by the University of Illinois and University of Puerto Rico groups that are working on the BTeV muon system.

The muon scintillation counters have been taken to the University of Illinois, repaired and roughly gain balanced using a radioactive source. Roughly 15% of the counters required repairs. A frame has been designed to hold these counters in an array that resembles the BTEV muon detector design. We believe we will have enough counters to either cover the full azimuth, or to cover half of the azimuth with two layers to suppress firings due to tube noise. We may be able to switch between these two configurations rapidly if the need arises.

7.7.9 Simulation and reconstruction work

A significant effort has already been expended on creating an accurate muon simulation in the BTeVGeant framework, including the complicated magnetic field resulting from having a dipole magnet inside a toroidal magnet. We plan to further verify these simulations by comparing with those obtained from inclusive simulations like MARS which include non-interaction region phenomena like beam scraping.

The BTeVGeant simulation was used to develop and evaluate the current dimuon trigger. Progress will continue on developing the dimuon trigger algorithm and hardware implementation. We will also investigate the effects of more noise, reduced efficiency, increased luminosity, geometry misalignments, etc.

We plan to work on developing full muon reconstruction code in order to be able to fully evaluate our misidentification rate and provide a better baseline for determining muon trigger efficiency. We also would like to investigate hybrid trigger schemes which utilize information from the muon system and vertex trigger to, for instance, trigger on beauty semileptonic decays more effectively than with the vertex trigger alone. These triggers would be implemented in the global level one trigger.

7.8 Production Plan

This section describes the plans for production, production testing, and production quality assurance of the BTeV muon system. The various components that need to be produced are (1) the sensor planes, which includes front-end electronics and cabling, and (2) support systems such as gas, low-voltage, and high-voltage. By far the largest task is the construction of the sensor planes, which will be built in modules at university sites (Illinois, Puerto Rico–Mayaguez, and Vanderbilt). These modules will then be delivered to Fermilab for installation. Our delivery, installation, integration, and shake-down plan (including the construction and installation of the mechanical support for the sensor planes) are described in the next section.

Octants mounted on octant plates are the basic installation unit of the muon system. An octant covers 1/8 of the azimuthal angle in one view, so there are 8 octants per view and 32 octants per station. Four octant plates are assembled into a wheel; two wheel make up a view.

Octant plates will be assembled at Illinois and Vanderbilt and shipped to Fermilab for installation there. A fully assembled octant plate will have all front-end electronics installed, as well as gas connections, low and high voltage cables, slow-control cables, and signal cables that are "interior" to the octant. When a octant is delivered to the C0 hall, it will only be necessary to attach it to the muon system mounting structure and make electronic, electrical, and gas connections to external devices (such as the experimental DAQ and to muon system low voltage supplies). The octant will have been fully tested prior to installation: all readout, electrical, and supply connections will have been verified at the octant assembly site prior to shipping.

For a one-arm muon system, there will be 3 detector stations, with 4 views per station, 8 octants per view, and 12 planks per octant. This results in 1,152 planks or 36,864 tubes (electronics channels). Planks range in length from 2 to 6 feet. We will build eight complete octants (96 planks, 3,072 tubes) during the pre-production stage (which we will use to shake down and evaluate our production lines and methods). During production we will make two additional views worth of planks to use as spares. These additional planks must be made at the same time to minimize the cost of the necessary parts and labor.

7.8.1 Construction overview

Muon octants will be fabricated at university sites and delivered pre-tested to Fermilab. Installation at Fermilab will involve attaching each octant to the support structure and connecting it to electrical, electronics, and gas. There are three main tasks in the construction of a octant: (1) plank fabrication, (2) front-end electronics fabrication, and (3) assembly of planks into octants.

7.8.1.1 Pre-production

In order to shake down and evaluate our production lines and methods, we will make eight pre-production octants. These octants will be fully instrumented so that we can fully debug and evaluate our testing and quality assurance program. This means that they will have a full complement of front-end electronics, gas supply lines, low and high voltage cables, slow-control cables, and readout cables. All of this "internal" cabling, as well as each of the proportional tube counters, will be tested and certified during the production process. Each of the plank production lines will fabricate planks during this pre-production stage, the electronics production process will be implemented, and the octants will be assembled at one or both of the octant assembly sites. Once the fabrication and testing of these octants is complete, we will evaluate all aspects of the process and make adjustments as necessary, and then begin the full production process of the full system.

7.8.1.2 Quantities of materials needed

The quantities of parts, planks, octants, etc., that must be acquired or fabricated are driven by the numbers listed in Table 7.3. For example, the total number of planks that will be installed in the base system can be determined by multiplying the planks/octant (12), octants/wheel (4), wheels/station (8), stations/arm (3), and arms/spectrometer (1), which gives 1,152. Multiplying this by tubes/plank (32) gives the number of proportional tube channels in the base system (36,864).

Manifolds, support ribs, gas connections, and Delrin inserts are all parts used to construct planks. The numbers given for these items in Table 7.3 are the number that will be in the base system. For example, there will be 2 Delrin inserts per proportional tube, or a total of 73,728 inserts.

The average tube length and longest tube are used in calculating the amount of tubing required. The remaining numbers in the table are important for calculating the total amount of materials (such as tubing) and parts that must be acquired/fabricated when accounting for spares, waste, mistakes, and so on. For example, the *fraction of problem planks* is our assumption of the number of finished planks that will be found to be bad by our quality assurance program (QAP). Once a plank is finished, it cannot be restrung or "rescued." If a plank is found to be bad, a new one must be made. So, if we need 100 planks, this fraction (0.1) predicts that we will have to make 110. Similarly, the *fraction of re-strung tubes* is an estimate of the number of tubes that have to be restrung because a crimp doesn't hold, the

Item	Value	Item	Value
Planks/octant (1 view)	12	Pre-production octants	8
Octants/wheel	4	Spare octants	16
Wheels/view	2	Fraction of problem planks	0.1
Views/station	4	Fraction of problem manifolds	0.1
Stations/arm	3	Fraction of problem support ribs	0.1
Arms (in the BTeV detector)	1	Fraction of problem Delrin inserts	0.1
Tubes/plank	32	Fraction of problem misc. parts	0.1
Manifolds/plank	2	Fraction of re-strung tubes	0.25
Support ribs/plank	2	Wire waste/tube strung (ft.)	2.5
Gas connections/manifold	2	Tube safety factor	2
Delrin inserts/prop. tube	2		
Average tube length (ft.)	4.1		
Longest tube (ft.)	6.5		

Table 7.3: Numbers and assumptions for the muon system. These determine the quantities of parts, planks, and octants that need to be fabricated. The meaning or derivation of these numbers is explained in the text.

tension is inadequate (too low), or the tube doesn't hold high voltage. The *wire waste per tube strung* is the amount of extra wire required when stringing a tube (1) to make sure the wire in the tube is clean and has no kinks, and (2) to connect to the tensioning part of the stringing apparatus. The *tube safety factor* is added because we don't know what lengths of planks will be bad and have to be re-made. We will buy the stainless steel tubes pre-cut to length, and will buy extra of each length to make sure we have enough of each of the required lengths. The "2" here does not mean we will buy twice as many tubes as needed, it means we will buy twice as many tubes as necessary to build all the bad planks, a 10% effect. These fractions and estimates are based on our experience stringing about 25 prototypes.

7.8.1.3 Pre-production and production quantities

Using the numbers in Table 7.3, we can calculate the number of parts, planks, and octants that must be acquired or fabricated. The resulting numbers are shown in Table 7.4. The calculations are based on two premises. First of all, it will be very difficult and expensive to get the assembly lines going to make planks, and to crank up production of the parts (manifolds, support ribs, Delrin inserts). Therefore, we must make all required quantities during production, and will not plan on going back and making more later. This means that all parts and materials, such as the stainless steel tubes for our proportional tubes, will be purchased during the production phase; it will not help to buy more later. Having to buy all necessary materials in advance complicates calculations of the required quantities. An example is the Delrin end plugs. We must have enough extra to account for re-stringing

	Pre-Production				Production					Sum
Item	Base	Bad Plnk	Re-string	Total	Instal-led	Spares	Bad Plnk	Re-string	Total	Total
Planks	96	10	0	106	1152	192	135	0	1479	1585
Tubes	3072	320	0	3392	36864	6144	4320	0	47328	50720
Octants	8	0	0	8	96	16	0	0	112	120
Gas manifolds	212	22	0	234	2535	423	297	0	3255	3489
Support Ribs	212	22	0	234	2535	423	297	0	3255	3489
Delrin End Plugs	6759	704	1866	9329	81101	13517	9504	26031	130153	139482
SS Tubing (feet)	12595	2080	0	14675	151142	25190	35424	0	211757	226432
Sense Wire (feet)	20275	2880	5789	28944	243302	40550	28512	78091	390456	419400
Crimp tubes	6759	704	1866	9329	81101	13517	9504	26031	130153	139482
Crimp wires	6759	704	1866	9329	81101	13517	9504	26031	130153	139482
Flare nuts	423	44	0	467	5069	845	594	0	6508	6975
Gas connect. tubes	423	44	0	467	5069	845	594	0	6508	6975

Table 7.4: Production quantities determined using the numbers and assumptions listed in Table 7.3.

(the plugs usually can't be saved), enough to re-make planks that are found to be bad after they are finished, and for plugs that are found to be defective after they are made. The second premise is that if a bad plank is found after it is completed (one of the wires breaks, or has insufficient tension), it will be very difficult to save the parts used to make it. A new equivalent plank will likely have to be made with all new parts. Fortunately, because of the tests we will perform on the tubes after they are strung and before they are assembled into a plank, we do not believe this will happen very often.

The derivation of some of the entries in Table 7.4 is trivial. For example, the number of *installed* planks in the production section is simply the number of planks needed for a working detector, as calculated in section 4.2 above. The number of *bad planks* is just the number we need to build (from the *installed* and *spares* columns) times the *fraction of problem planks* from Table 7.3. Others are less obvious. For example, the number of *installed* Delrin end plugs in the production section is the number needed for the detector plus the number we assume will be defective (see *fraction of problem Delrin inserts* in Table 7.3).

7.8.2 Plank fabrication

Plank fabrication involves several steps: acquire parts and materials, fabricate parts that need to be machined, string individual proportional tubes, test them, assemble the tubes into planks and test the planks, attach electronics to the planks, and test the planks in a cosmic ray test stand. Three plank fabrication lines will be established at Illinois, Puerto Rico, and Vanderbilt.

7.8.2.1 Parts of a plank

There are 11 different parts or materials needed to make a plank, not including the electronics. Each proportional tube will be made from a thin-walled (0.01 inch thick) **stainless steel tube** (3/8 inch in diameter) with a 30 micron gold plated tungsten **sense wire**. The sense wire is tensioned to 75% of its yield point, or 150 grams. A **Delrin insert** goes in each end of the tube to electrically isolate the wire from the tube and center the wire in the tube. It also has three gas holes. A **brass crimp tube** is inserted in each end plug, the sense wire exits the tube at each end through the plug and this tube. A thicker **crimp wire** is inserted into the crimp tube after the wire is threaded through, this helps the crimp hold the sense wire in place. Completed tubes are assembled into planks, which are held together at the ends by brass **gas manifold**s (see Fig. 1). For longer planks, the tubes will also be supported along their length by brass or aluminum **support ribs**, which will maintain the spacing of the tubes. The stainless steel tubes are glued into the manifolds at each end in two stages. In the first stage, conductive epoxy is used to provide an electrical connection and a modest amount of structrural support. In the second stage, the tubes are bonded to the brass manifold with structural epoxy. The potting done in this second stage provides the bulk of the structural support and a gas seal. The open end of the gas manifold is sealed by a **circuit board** with sockets on the inside that accept the brass crimp pins, these sockets will provide the signal connection to the front-end electronics. A brass sheet is glued (with conductive epoxy) or spot welded to the outside of the brass manifold to maintain electrical continuity and RF integrity. This sheet is soldered to the Front-end electronics to provide the ground connection for the signal and HV delivery. Two flared stainless steel (or brass) **gas tubes** will be glued into holes in each manifold, these will be connected to the gas supply lines with flare nuts.

7.8.2.2 Acquisition of materials and supplies

The materials needed to build the muon system planks should all be readily available stock items with the exception of the thin walled stainless steel tubes and the sense wire. These will require some lead time in purchasing (*i.e.* roughly 3 months before delivery of the first stainless tubes). The brass (including the crimp tubes) and Delrin required are standard stock items. Once delivery starts, all parts could be in hand in a matter of months. We may decide to stretch acquisition out for budgetary reasons, however.

7.8.3 Fabrication of manifolds, support ribs, and Delrin inserts

A major portion of the work required to build the planks needed for BTeV is fabricating the gas manifolds, support ribs, and Delrin inserts (which includes inserting the brass crimp pin). These three parts require substantial machining. The Vanderbilt Science Machine Shop will do the machining of the first two parts. The Vanderbilt machine shop has the computer controlled milling systems needed to make these parts in bulk already, and can make these parts substantially cheaper than a commercial shop. Fabrication of the Delrin inserts may be done by a commercial machine shop, or may be done in the Vanderbilt shop. For this part, commercial shops may be able to compete on price.

The manifolds and support ribs will require roughly two years to make. This is also roughly how long it will take to string and assemble all the planks, so the two will proceed in tandem. It will therefore be very important that the shop work be kept on schedule, so as not to delay the manpower intensive plank stringing operations.

7.8.3.1 Tube stringing and plank assembly

Plank stringing and assembly is the most labor intensive part of the muon system construction project. We have built roughly 25 prototype planks. Based on this experience, we have produced Table 7.5, which breaks plank assembly into sub-tasks and estimates the time and personnel required to perform each.

The times in Table 7.5 are under "optimal" conditions, in which we have the parts required and the operation is running smoothly. In estimating our total required labor, we increase the total time per plank by 15% to account for inefficiencies. We also increase the time required to make the first few planks because we assume it will take some time to "ramp up" to smooth operation of the assembly lines. We assumed it would take twice as much time for each production line to make their first 3–4 planks. The total times for the pre-production and production runs are summarized in Table 7.6. These numbers can be divided by 3 to get the times for each institution.

Individual tubes will be strung in a stringing jig. This is a two person operation. After stringing and testing, the gas manifolds that go on each end of a plank are assembled with 32 tubes, and this assembly is then glued together. A G10 circuit board is epoxy potted onto the open end of each gas manifold. The circuit board also connects to the individual sense wires and provide the signal path to the front-end electronics. Finally, a small brass sheet is glued to the end of the brass manifold with conductive epoxy for ground conveyance and noise suppression.

Once the G10 circuit boards are in place, the front-end electronics and the interface cards are attached, and the plank is ready for the cosmic ray test stand and, if it passes our QAP, is ready to be assembled into octants.

Each site will produce one plank per day on average. This includes all testing and assembly.

Task (times are in hours)	Time	UG	Grad	PD	Tech	Facul.
Project management/supervision	0.50					0.5
Wash and prep tubes	0.50	0.40	0.10			
Wash and prep machined parts	0.50	0.40	0.10			
Wash and prep other parts	0.20	0.20				
QAP: Inspect parts after prep, add bar code	0.20			0.20		
String tubes, includes restringing	6.00	2.00	3.00		1.00	
QAP: Visual inspect strung tubes	0.10			0.10		
QAP: Individual tube tension measurement	1.00		1.00			
QAP: HV test in air (meas. current at 1.5 kV)	0.50	0.50				
QAP: Inspect tension/HV results	0.10			0.10		
Glue plank together	4.00		2.70	0.30	1.00	
Glue circuit board end cap to manifolds	1.20		0.90	0.10	0.20	
Glue gas connections tubes in	0.50	0.50				
Attach electronics	1.00		0.70	0.10	0.20	
QAP: Gas leak test	0.50		0.50			
QAP: Plank tension measurement	1.00		1.00			
QAP: Visual inspection	0.10			0.10		
QAP: Cosmic ray test stand, analyze data	2.00		1.00	1.00		
TOTALS	**19.90**	**4.00**	**11.00**	**2.00**	**2.40**	**0.5**

Table 7.5: Plank assembly sub-tasks and the labor and personnel required for each. These times are for the fabrication of one plank. UG stands for undergraduate student, PD means post-doc.

Task (times are in days)	Time	UG	Grad	PD	Tech	Facul.
Pre-prod times incl. inefficiency	337.55	67.85	186.59	33.93	40.71	8.48
Prod. times incl. inefficiency	4256.61	855.60	2352.90	427.80	513.36	106.95

Table 7.6: Labor required to make all pre-production and production planks.

7.8.3.2 Plank Quality Assurance Program (QAP)

Tests and measurements are performed at all stages of plank production as a part of our quality assurance program.

After each proportional tube is strung, it is tested for continuity and to see if it has slipped out of the crimp at either end (and is shorted to the tube walls). The wire is re-strung if a problem is detected. Then the tube is tested to verify that it will hold high voltage (1600 Volts) in air, and the wire tension is determined by finding the resonant frequency of the wire in a uniform magnetic field when a variable frequency AC current is applied to the wire. If any tubes are out of tolerance or fail outright, they will be re-strung.

Once the tubes are glued together into planks and the G10 circuit board end is glued into place, we will retest the tension of each wire and do a leak test on the plank. If the plank passes these tests, the plank will be installed in a cosmic ray test stand and we will do plateau curves and measure efficiencies and noise rates for each tube. An inventory control system based on bar codes will be used at all points during the construction. Information such as test results, parts used, and the personnel performing the work will all be recorded in a database associated with the bar code that will be attached to each tube and to each plank. A bar code reader will be used to scan in the bar code on each plank or tube. Additional information will be entered via easy to use computer interfaces which will be tailored for each step in the process. Each front-end electronics card will also have a bar code label. Information on which electronics card is associated with which plank, and which tubes are associated with which plank, will be logged and modified as changes are made.

7.8.4 Electronics QAP

It is essential to identify electronics problems as early as possible. All fabricated ASDQ chips are tested before they are used in the circuit board assembly. The tests are well understood and were used by the University of Pennsylvania during the ASDQ vetting process for the CDF production. The expected yield and additional costs for testing are included in our cost estimate. All fabricated circuit boards must pass an electrical test at the fabricator's location. All stuffed circuit boards will be programmed at the end of the assembly process by the assembler and a power-up go or no-go will be indicated. This allows us to identify production problems early. Once assembled boards arrive at Vanderbilt, they will be placed in a fixture that mimics the electrical environment we expect during data taking. Any errors will be noted, and no boards that are less than 99% efficient will be allowed to be placed on a plank. The cards that interface the ASDQ-FPGA boards to the detector will be continuity and high-pot tested at 2000 V before being mated with the planks and the ASDQ-FPGA boards.

7.8.5 Octant assembly and QAP

The detector modules (octants) will be assembled from the planks at both Illinois and Vanderbilt. Puerto Rico may participate at this stage if it can be shown that shipping the

octants from there is not prohibitively expensive. The planks for each module will be held together by attaching them to pre-drilled and slotted 1/8" aluminum sheets called octant plates.

The internal signal, gas, and HV connections will be established as the octant is assembled. These connections will be verified in an octant test stand which will provide gas, control signals, and low and high voltages to all planks in the octant. We will verify that each channel (proportional tube) is operating as expected and that it can be read out. Once complete, each octant will be packed and readied for transport to Fermilab. A portion of the octant plate which is not used for mounting planks can be removed to facilitate shipping if convenient (see Fig. 7.6).

7.9 Installation, Integration and Testing Plans (at C0)

This section describes the installation, integration and testing plans for the BTeV muon system. As described above, the octants shipped to Fermilab will already have undergone a rigorous testing and quality assurance program at the production sites. They will be ready for installation and, unless they are damaged in shipment, ready to go.

7.9.1 Transportation of muon detector octants to C0

The octants will be delivered to C0 as they are fabricated at the production sites. They will be stored at C0 or some other appropriate place, and installed during periods in which we have extended access to the hall.

7.9.1.1 Equipment required

The octants which will be shipped to Fermilab will be too heavy to carry reliably without assistance. A roller cart will be required to move them. The required carts will be built in the Illinois machine shop and shipped to Fermilab and the other octant production site at Vanderbilt University. The octants will be shipped to Fermilab; we are still working out how this will be done. We will either rent trucks and move them ourselves, or ship them with a commercial carrier.

7.9.1.2 Special handling

The proportional tubes that make up the muon system will be made from stainless steel tubes strung with 30 micron gold-plated tungsten wire. The wires will be held in place with by crimped brass tubes at each end. The planks themselves will be extremely sturdy and strong, and the electronics and other connections internal to the octant will be very robust. The concern with the detectors is that some of the crimps holding the wire in place will fail or that wires will break, especially during shipping. This will be our major concern in determining how we will move the octants to Fermilab.

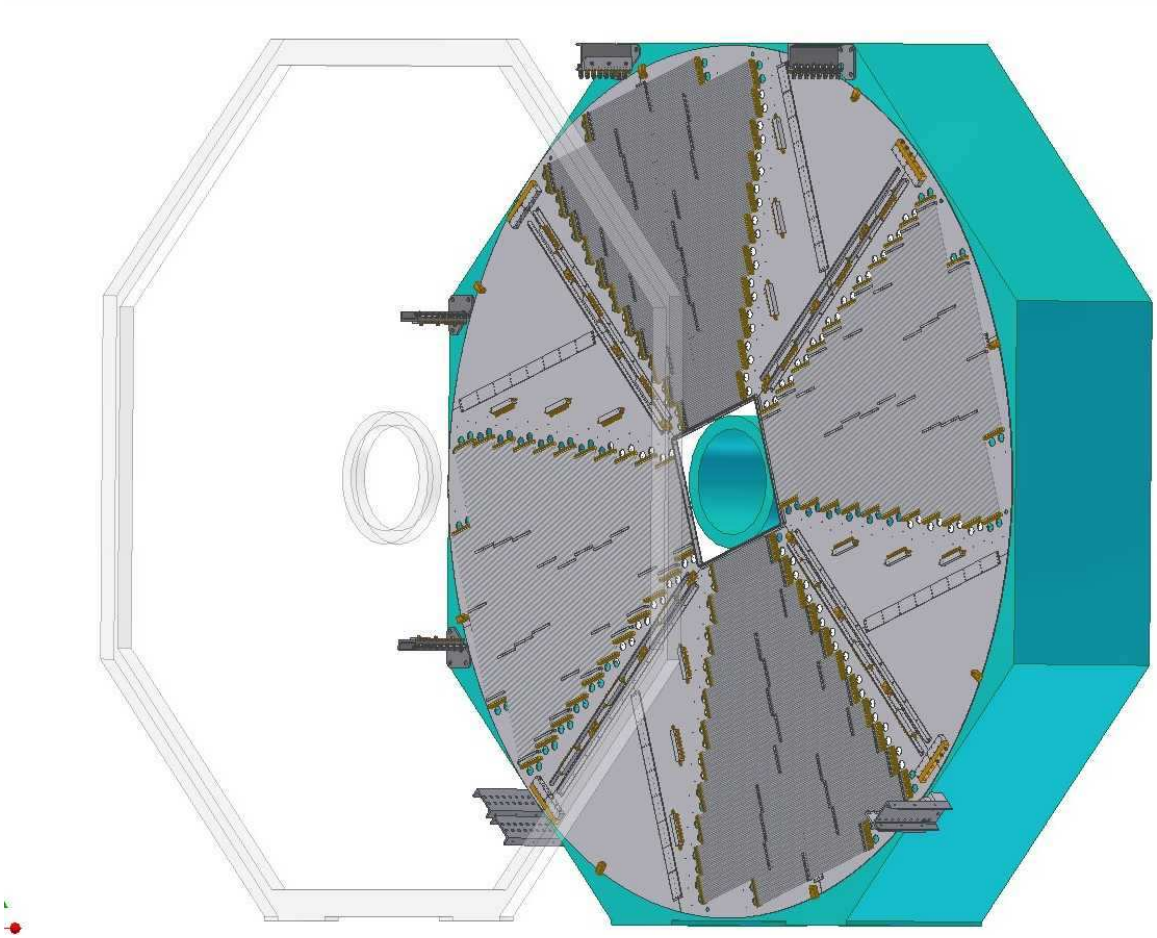

Figure 7.24: The mounting wheel will be supported from beams attached to the toroid. The upper two beams will support the $\approx$ 1500 lb weight of each wheel, the additional beams will prevent the wheel from swaying.

7.9.2 Installation of muon system elements at C0

The muon octants are designed so that they can be inserted from the wide aisle side of the detector hall. One dynamically creates a mounting "wheel." The first octant plate is inserted from the side and then rolled to the bottom position on a series of rollers that contact the octant plate circumference. The next octant plate is then attached to the previous plate using specially designed knitter brackets. One then rolls the two octant partial wheel into a position that allows the attachment of the third plate. Once all 4 plates of a wheel are assembled, the wheel is lifted off of the floor and mounted from beams attached to the toroid, as illustrated in Fig. 7.24 and the floor wheels (bogies) are removed and used for the installation of the next wheel. In all, 8 wheels are used for each station.

The process can be reversed for repairs. In the worse case, the replacement or repairs of

a single plank will require de-cabling its wheel and sequential dismounting and rotation of the wheel until the affected octant is in a convenient position for repairs.

7.9.2.1 Installation steps

Testing of octants on arrival: When the octants arrive at C0 from the production sites, we will retest them with the same test system used at the production sites: testing gas flow, current draw, readout of all channels, etc. Any problems will be fixed.

Installation of octant support structure: The octants will then form "mounting wheels" during installation. These mounting wheels will be supported from the sides and top of the toroid and filter using a set of specially designed hangers which attach to fixtures on the wheel assembly.

Installation of relay racks, gas system, and other support infrastructure: We assume that the installation of relay racks and other support infrastructure (such as the gas system) will occur as early as possible. Low voltage and high voltage supplies, as well as data acquisition hardware, can be installed as needed (*i.e.* as new octants requiring them are installed, if possible).

Suspension of octants: The mounting wheel will be supported from beams attached between the toroids. The upper two beams will support the $\approx$ 1500 lb weight of each wheel as shown in Fig. 7.25. Additional beams will prevent the wheel from swaying. In principle, the muon system can roll with the toroid if one needs to move the toroids to service accelerator magnets.

We plan to install over a long period of time, as octants become available, and during extended shutdowns.

Low and high voltage, DAQ hardware installation: These items will hopefully be available as needed, *i.e.* as new octants are installed. We will install them at the same time as their corresponding octants, or ahead of time if they are available.

Connection of electrical, gas, and electronics: Once all the octants in a wheel are installed we make all gas, electrical, data acquisition, and slow control connections. We will then proceed to test these connections as described below.

7.9.2.2 Equipment required

For installation, special rigging will need to be assembled; again this will be provided by Illinois. This is envisioned as a special installation arm and guide rod that attach to an octant. A rail and pulleys will then allow manipulation of each octant as it is being positioned into its mounting wheel.

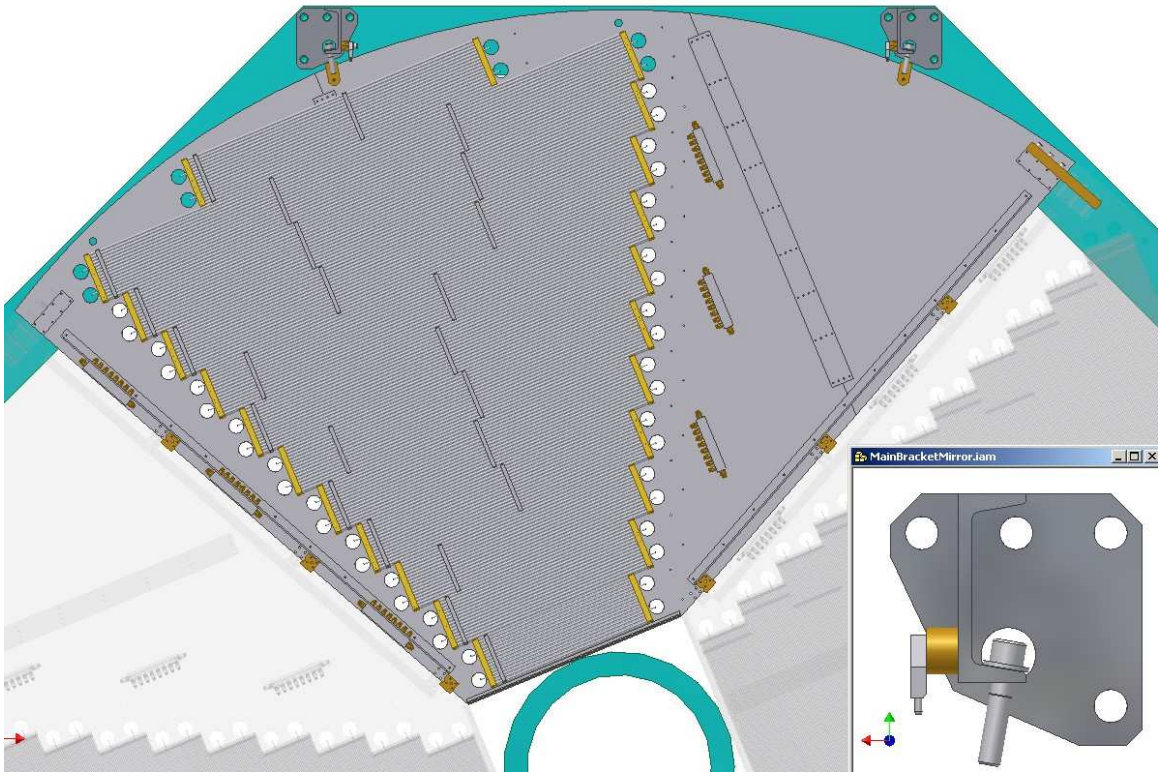

Figure 7.25: Details of the hanging brackets used to support the octant plate wheel assemblies.

7.9.2.3 Personnel required

The octants will be installed by members of the muon group. However, the support structure (beams) for the views will need to be installed by Fermilab personnel (welders, riggers,...). In addition, DAQ personnel may be needed to help with connection of the octants to the DAQ.

7.9.2.4 Time required

We estimate that it will take up to 12 hours to install each wheel of 4 octants, which translates to 4 days per station or 12 days for the full detector. This does not include connections, which we estimate will take an equal amount of time. We believe the time to install octants will decrease as we get better at it. Note that in real time this will take roughly two years, as we plan to install octants as they become available and as opportunities exist to gain access to the experimental hall for extended periods. The first octants should start arriving at C0 in late 2006. The final octants should be ready by the summer of 2008.

7.9.3 Testing of muon system elements at C0

7.9.3.1 Stand-alone subsystem testing

Mechanical: As each octant is installed, the gas system will be tested for leaks and proper flow.

Electrical/electronics: As each octant is installed and connected, we will (carefully) bring them up to voltage and verify that they are drawing the expected current. We will check a channel or two in each plank with a scope to verify that they seem to be behaving as expected (expected noise level, signals look OK, etc.). We will then readout each channel and verify that each is connected to the DAQ and functioning as expected.

Software: When a view is installed, we should be able to look for cosmic rays, and to look at beam background when the accelerator is on. As we add views to each station, we can start to do more sophisticated tests and can start to debug our readout software, reconstruction software, and the muon trigger. We may determine the installation order to make best use of these kinds of tests.

Personnel required: Muon group (and muon trigger group) personnel can perform all stand alone testing, although some interaction with the DAQ and trigger groups will be important.

Time required: This activity will go on over an extended period of time (two years), as described above. This will give us plenty of time to debug our software and to perform multiple tests; we should not have a problem keeping up.

7.9.3.2 Combined systems testing

Electrical/electronics/readout/software: We hope to be using the DAQ early on, even in our "stand alone" tests. We also hope to use these tests to debug the muon trigger. So, the above "stand alone" tests will also be integration tests with the DAQ and trigger, two important elements that we connect with. We also will want to investigate higher level triggering, which will require information from the tracking systems. Once the tracking systems become available, we will start these tests.

Personnel required: Muon group (and muon trigger group) personnel will participate. Some interaction with the DAQ, trigger, and tracking groups will be required.

Time required: This activity will go on over an extended period of time (two years), as described above. This will give us plenty of time to debug our software and to perform multiple tests; we should not have a problem keeping up.

	Station 1	Station 2	Station 3	Total
Average number of hits per crossing	42	8	9	54
Average occupancy	0.34%	0.06%	0.07%	0.15%
Maximum channel occupancy	2.5%	0.24%	0.52%	
Maximum plank occupancy	1.6%	0.17%	0.31%	

Table 7.7: Muon detector occupancies obtained from BTeVGeant simulations with an average of 2 minimum bias interactions per crossing and a crossing rate of 7.6 MHz (132 ns bunch spacing). These numbers should be multiplied by 3 for 396 ns bunch spacing. Average occupancy is the occupancy of the detector in a single crossing. Maximum channel occupancy is the maximum hit rate for the innermost channel. Maximum plank occupancy is the average per channel hit rate of the innermost plank.

7.9.3.3 Completion of commissioning

The muon detector will be considered fully commissioned when the entire system is under voltage, gas is flowing, and near-horizontal hits from cosmic rays or beam backgrounds are able to be read out through the DAQ.

7.10 Performance

Extensive simulations of this detector as well as previous iterations have been performed. These simulations use BTeVGeant which is based on GEANT3. These simulations have been used to help determine the best geometry, shielding scenarios, etc. The simulations have also been used to develop and validate the dimuon trigger.

The BTeVGeant simulations include a full tracing of particles produced by signal and minimum bias interactions at the nominal luminosity of $2 \times 10^{32}\text{cm}^{-2}\text{s}^{-1}$. This tracing includes decays, hadronic and electromagnetic interactions, multiple Coulomb scattering, etc. The full BTeV detector geometry is used including beam pipes and support structures, as well as detector elements. The magnetic field in the muon region includes the effect of the muon toroids and the compensating dipole and is calculated with the POISSON program. The muon proportional tube response to charged particles is to fire if a particle passes within 85% of the inner radius of a tube.

7.10.1 Occupancies

At our nominal luminosity of $2 \times 10^{32}\text{cm}^{-2}\text{s}^{-1}$ and a minimum bunch spacing of 132 ns, we expect 2 minimum bias interactions/crossing which are simulated using a Poisson distribution with mean of two. Table 7.7 and Fig. 7.26 summarize the detector occupancies obtained from BTeVGeant under this scenario. These occupancies should be mulitplied by 3 for operation at 396 ns between crossing and an average of 6 interactions/crossing. Even at 396 ns, these occupancies and rates are fairly low by modern detector standards.

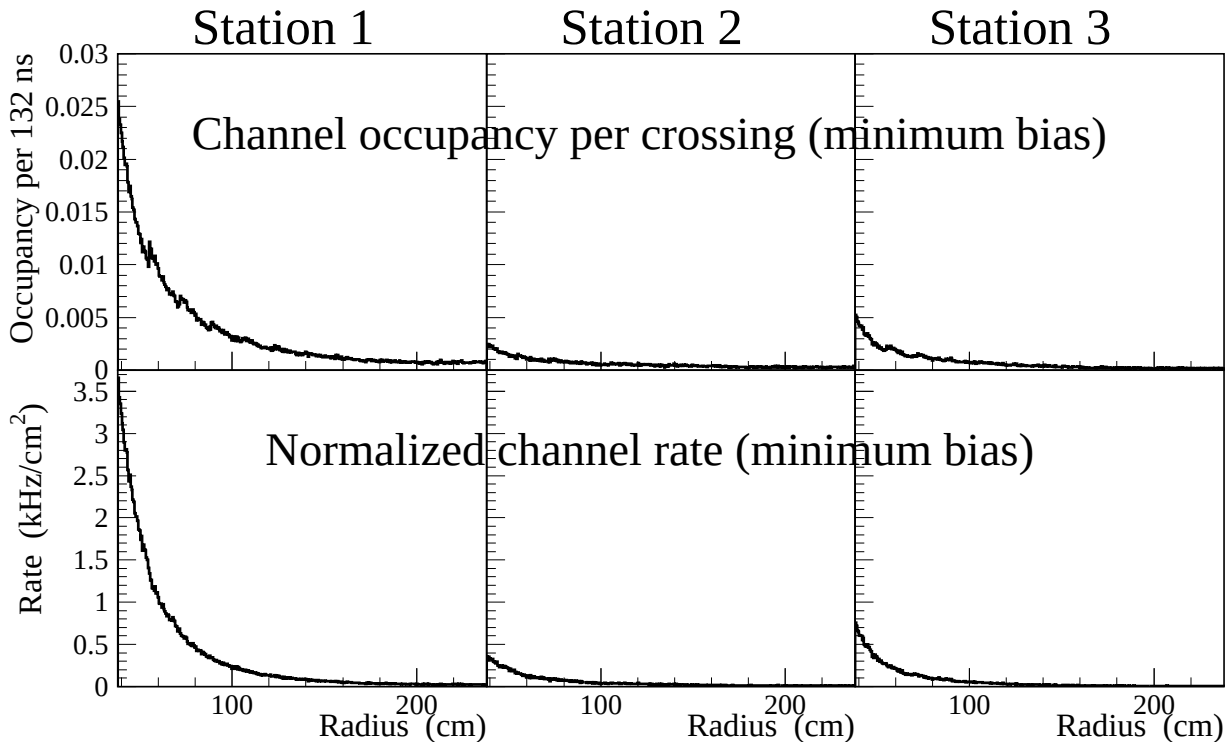

Figure 7.26: Radial distributions of tube occupancies (top) and normalized rate (bottom). These results are from the first radial view in each station, averaged over the eight octants.

7.10.2 Dimuon trigger

The muon trigger is described in more detail in Chapter **??**. However, a major goal of the muon detector is to be able to generate a stand alone dimuon trigger and therefore the design and performance of the muon detector and trigger are closely related. The University of Illinois has designed a simple trigger which can be easily implemented using Field Programmable Gate Arrays (FPGA) and Digital Signal Processors (DSP). The trigger development started by noticing that good muons are well described by the equation $R2 = a + bR1 + cR0$ where a, b, and c are constants and $R2, R1, R0$ are the numbers of the tubes hit by a good muon. This equation describes a plane in the 3-dimensional space defined by $R0$, $R1$, and $R2$. Four of these equations are generated (one for each view). In each view a muon candidate is found when three hits match the equation (within a user definable error). If three out of four views find a muon candidate (of the same sign) then a good muon is found. In this algorithm, each octant is treated independently. The dimuon trigger is satisfied if two good muons of opposite sign and from different octants are found. Two muons which travel through the same octant or a muon which crosses octants will be lost by the trigger.

The University of Illinois group used the results of BTeVGeant simulations to tune this trigger and determine efficiency for signal and rejection of background. The signal mode is $B^0 \to J/\psi K^0_S$ where $J/\psi \to \mu^+\mu^-$. The background is minimum bias. The signal and

background events are generated assuming 2 interactions/crossing. The trigger algorithm described above can obtain an efficiency of 80% with a rejection rate of 500:1 which is well above our design goals of 50% efficiency with a rejection rate of 300:1. Here, efficiency is relative to all events where both muons pass through all three muon chambers and the rejection rate is the inverse of the minimum bias efficiency. More severe running conditions such as 3–4 interactions/crossing and tube efficiencies as low as 95% still give a broad range of options for greater than 50% efficiency with a rejection rate better than 500:1. Details of these studies and their relevance to running with a bunch spacing of 396 ns can be found in Section **??**.

7.11 Test Results

In the summer of 1999 we conducted our first test beam run using our first prototype of the detector and electronics. The tubes were quite efficient but susceptible to external RF noise and cross talk. This led us to redesign the high-voltage distribution card, construct the manifolds out of brass (conductor) instead of Noryl (insulator), and electrically connect the manifold to the tubes providing a Faraday cage. Also, a newer version of the amplifier/shaper/discriminator (ASD) chip is now being used. After several iterations we now have a design, described above, which we have proven can be built and provides the necessary capability. It has been tested in a cosmic ray test stand at Vanderbilt. We find tube efficiencies above 99% with a gas of 85:15 Ar–CO_2. The noise level is consistent with the inherent noise of the ASD chip and the cross talk is negligible. We have run the new planks in a test beam during the summer of 2003 and verified the improved performance over the 1999 prototypes. We plan to produce prototypes incorporating all of our production techniques and new electronics and test these new planks in a test beam in February of 2004.

Bibliography

[1] J. Wiss, BTeV-doc-970, http://www-btev.fnal.gov/cgi-bin/DocDB/ShowDocument?docid=970

[2] P. Sheldon and K. Stenson, BTeV-doc-991, http://www-btev.fnal.gov/cgi-bin/public/DocDB/RetrieveFile?docid=991)

[3] J. Wiss, BTeV-doc-3405, http://www-btev.fnal.gov/cgi-bin/DocDB/RetrieveFile?docid=3405)

This document is BTeV-doc-1874. The version in the DocDB may lag behind; the most up to date version can always be generated from the CVS repository by running "buildMuon" in the part-3 directory

References to other chapters may appear to be broken in this document, but when building the full TDR, they will appear correctly.